Conformational Dynamics of Helix 10 Region as An Allosteric Site in Class A β-Lactamase Inhibitory Binding

Liwen Huang[1], Pui-Kin So[1], Yu Wai Chen[1], Yun-Chung Leung[1], Zhong-Ping Yao[1,2*]

[1]State Key Laboratory of Chemical Biology and Drug Discovery, Food Safety and Technology Research Centre and Department of Applied Biology and Chemical Technology, The Hong Kong Polytechnic University, Hung Hom, Kowloon, Hong Kong Special Administrative Region, China

[2]State Key Laboratory of Chinese Medicine and Molecular Pharmacology (Incubation) and Shenzhen Key Laboratory of Food Biological Safety Control, Shenzhen Research Institute of The Hong Kong Polytechnic University, Shenzhen 518057, China

ABSTRACT: β-Lactamase inhibitory protein (BLIP) can effectively inactivate class A β-lactamases, but with very different degrees of potency. Understanding different roles of BLIP in class A β-lactamases inhibition can provide insights for inhibitor design. However, this problem was poorly solved based on the static structures obtained by X-ray crystallography. In this work, ion mobility mass spectrometry, hydrogen deuterium exchange mass spectrometry and molecular dynamics simulation revealed the conformational dynamics of three class A β-lactamases with varying inhibition efficiency by BLIP. A more extended conformation of PC1 were shown compared to TEM1 and SHV1. Localized dynamics differed in several important loop regions, i.e., the protruding loop, H10 loop, Ω loop and SDN loop. Upon binding with BLIP, these loops cooperatively rearranged to enhance the binding interface and to inactivate the catalytic sites. In particular, unfavorable changes in conformational dynamics were found in the protruding loop of SHV1 and PC1 showing less effective binding. Intriguingly, single mutation on BLIP could compensate the unfavored changes in this region, and thus exhibited enhanced inhibition towards SHV1 and PC1. Additionally, the H10 region was revealed as an important allosteric site that could modulate the inhibition of class A β-lactamases. It was suggested that the rigid protruding loop and flexible H10 region might be determinants for the effective inhibition of TEM1. Our findings provided unique and explicit insights into the conformational dynamics of β-lactamases and their bindings with BLIP. This work can be extended to other β-lactamases of interest and inspire the design of novel inhibitors.

Introduction

Antibiotic resistance has become a global concern during the past decades. Among the various classes of antibiotics, β-lactam antibiotics are widely used in clinical practice but severe resistance against them by β-lactamase-producing bacteria has emerged. β-lactamases are a group of key enzymes with extremely high efficiency to hydrolyze β-lactam antibiotics. To overcome the antibiotic resistance, several small-molecule inhibitors, e.g., clavulanic acid, sulbactam and tazobactam, have been developed to suppress the activities of β-lactamases and are used in combination with antibiotics to treat bacterial infection. However, due to the extensive use of these inhibitors, bacteria have been developing resistance towards them by producing inhibitor-resistant β-lactamases. Therefore, it is highly desirable to develop alternative strategies to inhibit β-lactamases. [1]

Among all classes of β-lactamases, class A β-lactamases are predominantly identified in clinical isolates for both Gram-negative and Gram-positive bacteria.[2] The TEM-type and SHV-type class A β-lactamases are most clinically prevalent and have evolved into hundreds of variants, some with abilities to confer resistance to inhibitors.[3] In this study, we focused on three parental class A β-lactamases, i.e., *Escherichia coli* TEM1, *Klebsiella pneumoniae* SHV1, and *Staphylococcus aureus* PC1 (see Fig. 1a for their aligned sequences). These enzymes share high sequence identity and structure similarity, especially between TEM1 and SHV1 (Fig. 1). β-

Lactamase inhibitory protein (BLIP), which is naturally produced by soil bacterium *Streptomyces clavuligerus*, is a unique inhibitor for β-lactamases and shows particularly high inhibition potency towards TEM1. Intriguingly, it inhibits SHV1 and PC1 with much lower efficiency (Fig. 1c). In addition, the inhibition potencies of BLIP towards SHV1 and PC1 can be considerably improved by point mutations on BLIP, i.e., E73M and K74G, respectively.[4,5] Hence, BLIP can be a highly potential inhibitor towards various β-lactamases and offers an unusual and alternative way to overcome inhibitor resistance. In this regard, understanding the properties of interactions between BLIP and these β-lactamases is highly important for further development of novel BLIP-related therapeutic agents.

The crystal structures of β-lactamases TEM1, SHV1 and PC1 have been revealed.[6–8] A typical class A β-lactamase comprises of two domains, including a five-stranded antiparallel β-sheet domain, and an entirely α-helical domain that packs against the β-sheets from the first domain (Fig. 1b). The catalytic-site Ser70 serves as the nucleophilic amino acid, which is located at the interface of these two domains.[9] The catalytically important residues, including Ser70, Lys73, Ser130, Glu166 and Lys234, form an active pocket in catalysis. The crystal structure of BLIP (PDB ID: 3gmu) has been solved,[10,11] and its complexes with TEM1 (PDB ID: 1jtg) and SHV1 (PDB ID: 2g2u) have been extensively studied.[12,13] Particularly, eight β-strands from BLIP pack together to form a concave surface that accommodates the protruding loop on the β-lactamases and the β-hairpin loop on BLIP inserts into the active cavity of β-lactamases (Fig. 1b). Structural alignment of TEM1 (PDB ID: 1btl) and SHV1 (PDB ID: 1shv) showed highly similar structures, with a root mean square deviation (RMSD) in all-atom positions of 1.5 Å, and the RMSD of TEM1 (PDB ID: 1jtg) and SHV1 (PDB ID: 2g2u) after binding decreased to 1.1 Å, showing highly similar binding modes (Fig. 1c).

The broad range of inhibition potencies of BLIP towards different β-lactamases has attracted considerable research interests in studying the factors governing these inhibitory bindings and developing evolutionary BLIP variants with improved inhibition efficiency.[14–18] Regardless of extensive studies on this field, our understandings on the interactions between BLIP and β-lactamases have been mainly based on the static picture of the stable forms of the inhibitory interactions. The conformational dynamics,[19,20] which could be determinant to differentiate the binding interactions of these "similar" β-lactamases, has been seldom explored. Ion mobility mass spectrometry (IM-MS) can sensitively probe the conformational changes of molecular ions in the gas phase,[21] while hydrogen deuterium exchange-mass spectrometry (HDX-MS) has been widely applied to study protein dynamics by examining the exchange of amide hydrogen with deuterium in solution.[22–25] Molec-

ular dynamics (MD) simulation is a powerful tool for exploring the complexity of protein molecules, especially in protein dynamics, thus providing complementary information to experimental studies.[26,27]

In this study, we integrated IM-MS and HDX-MS with MD simulation to synergistically elucidate the mechanism of inhibitory interactions between three representative class A β-lactamases and BLIPs. Particularly, natural variants of class A β-lactamases here allowed investigation of the effects of extensive simultaneous mutations and large conformational rearrangements on inhibitory binding. Furthermore, BLIP mutants with enhanced binding affinity confirmed the changes in conformational dynamics regarding the inhibition of these β-lactamases.

Results and discussions

Global conformations of class A β-lactamases revealed by IM-MS and HDX-MS. The β-lactamases were characterized by mass spectrometry under denatured (50% acetonitrile with 0.2% formic acid) and native (100 mM ammonia acetate) conditions (Fig. S1). The mass spectra obtained for TEM1/BLIP, SHV1/BLIP and PC1/BLIP under native conditions confirmed the formation of the complexes with the binding ratio at 1:1 (Fig. 2a). The deconvoluted masses for the complexes TEM1/BLIP, SHV1/BLIP and PC1/BLIP were 48076.0±1.6 Da, 47910.3±0.5 Da, and 48094.8±0.4 Da, respectively, which were consistent to the expected values.

Ion mobility of the free β-lactamases was performed to compare their native conformations. Their arrival time distributions at charge states 10+ were shown in Fig. 2b. The drift time of TEM1 and SHV1 was similar but shorter than that of PC1, indicating that PC1 displayed a more extended conformation than TEM1 and SHV1 in the gas phase. After the β-lactamases bound to BLIP, the complexes at charge state 14+ displayed little difference in drift time distribution. Such observation indicated similar conformations among the class A β-lactamases after binding BLIP. These results are consistent to the crystal structures (PDB IDs: 1jtg and 2g2u) that show little conformational differences among these homologous protein complexes.

The conformational dynamics was measured for the free and BLIP-bound states of intact β-lactamases. We compared the global HDX profiles spanning 10 sec, 60 sec, 10 min and 60 min for the three β-lactamases in solution (Fig. 3a). The deuterium uptake for TEM1 was higher than that for SHV1 and PC1. The difference in global HDX profiles indicated that the flexibility of backbone amide hydrogens for TEM1 was higher, reflecting that the overall structures of SHV1 and PC1 could be more rigid than that of TEM1. After inhibitory binding by BLIP, all β-lactamases showed similar HDX profiles that corresponded to similar flexibility of the bound states. Interestingly, the conformational changes for TEM1 in-

duced less deuterium uptake, indicating stabilized conformations after the binding. These observations might also indicate that the higher affinity of BLIP for TEM1 than SHV1 and PC1 could result from a more dynamic unbound state.[28]

Unraveling the local flexibility of key regions in class A β-lactamases. Local HDX was performed by on-line pepsin digestion of the exchanged proteins followed by LC-MS analysis, with the sequence coverage as shown in Fig. S2. The H10 region showed fast deuterium exchange (indicated in red in Fig. 3b), reflecting very flexible structures for these class A β-lactamases. The fragment covering residues 211-225 from TEM1 underwent significantly faster deuterium uptake than that from SHV1 (Fig. 3b). From the available crystal structures (PDB IDs: 1btl and 1shv), it was observed that the H10 region of SHV1 showed the largest deviation (2.5 Å) from that of TEM1 compared to the other regions. Comparing the corresponding regions of the three β-lactamases, in TEM1 residues 211-225 comprise a loop between two helices, whereas in PC1 three residues 218-220 form a 3/10-helix (PDB ID: 3blm); and in SHV1, seven residues 218-224 form an α-helix. Helix, known as an ordered secondary structure, can protect amide hydrogen from deuteration.[29] The corresponding segment in SHV1 had the most helical structure and thus gave the slowest deuterium exchange, which was consistent with our HDX-MS results.

The deuterium uptake of the N-terminus of protruding loop (residues 92-104) for TEM1 was significantly less than that for SHV1 and PC1, reflecting a more ordered structure for TEM1 (Fig. 3c). By contrast, this loop on PC1 was the most flexible. It should be noted that the residue at position 104 for TEM1, SHV1, and PC1 is Glu, Asp, and Ala, respectively, with a decreasing size of side chain. Such variation might explain the difference in flexibility of this loop. Furthermore, it has been reported that the protruding loop comprises of the major binding interface with BLIP,[9] thus differentiated flexibility of this loop could be important for the accommodation onto the binding interface.

Interestingly, the HDX profiles of SDN loop and C-terminus of Ω loop for TEM1 and SHV1 were similar while those for PC1 were different from TEM1 and SHV1 (Fig. 3c). This is consistent with the similar substrate specificities for TEM1 and SHV1. In contrast, the results indicated that these loop regions on PC1 show different conformational dynamics from those on TEM1 and SHV1. Such observation supported that PC1 exhibited different substrate specificity from TEM1 and SHV1.[30,31] The difference might also contribute to the varying inhibition potencies by BLIP since the Ω loop plays an important role in the binding pocket of class A β-lactamases.

Cooperative binding interactions between the TEM1 β-lactamase and BLIP. Briefly, we found that the protein was considerably protected from deuterium exchange after binding with BLIP (Figs. 4a & b).

The protruding loop-covering fragments 82-101 and 101-118 from TEM1 showed around 15% decrement in deuterium uptake. Such obvious change strongly supported that this loop could be the predominant binding interface with BLIP, which has been proven by the crystal structure of TEM1-BLIP complex.[9] In this structure (PDB ID: 1jtg), the protruding loop of TEM1 and the concave sheet of the inhibitor form a concave/convex interface in the complex. Our study supported that this binding interface includes the protruding loop, and further analyzed the changes in dynamics at the residue level by comparing the overlapping fragments.[32] By subtracting the deuteration of these overlapped fragments, it was shown that residues 102-105 on TEM1 were unprotected from deuterium exchange in the free state while Val103, Glu104, and Tyr105 were under protection in the bound state. This protection corresponded to the hydrogen bonding network between TEM1 and BLIP as calculated from the crystal structure.[9] The protection of Val103 might be due to the reduced solvent accessibility since this residue interacted with Trp112 and Trp162 (both from BLIP) via van der Waals forces. By contrast, Glu104 and Tyr105 were protected mainly because of both the hydrogen bonding and van der Waals interaction with residues from BLIP. Hence, the protection of Glu104 and Tyr105 was more considerable than that of Val103. Previous studies revealed that a single mutation Asp104Glu for SHV1 could result in a 1000-fold enhancement in binding affinity with BLIP, indicating the important role of Glu104 in this inhibitory interaction. This enhancement was proposed to be explained by the restoration of a salt-bridge between Glu104 and BLIP Lys74.[18] Tyr105 was also investigated by mutagenesis, which showed that substitution of this position could cause inhibitor resistance due to oxyanion hole distortion.[33] Our observations from MD simulation showed that reduced fluctuation was observed for Glu104 and Tyr105 but not for Leu102 and Val103 after the inhibition (Fig. S3). Taking these together, our results revealed the important role of the dynamics of Glu104 and Tyr105 in the inhibitory binding.

The H10 region, which was found to be the most flexible region in free TEM1, showed a remarkably reduction in deuterium uptake after the binding, indicating that this region was involved in the binding interaction. Fragment 214-221 showed more than 20% decrement for both 1 and 10-min exchange upon BLIP binding. This change was the most significant among all the identified fragments. Combining the exchange profile of fragments 210-221, 211-221, 212-221 and 214-221, we estimated the deuterium uptake for residue 211, 212 and 213-214, and found that residues 211-214 were not involved in the binding (Fig. S4). In contrast, residues 215-221 were responsible for the inhibitory interaction. Trajectory analysis of these residues confirmed that Lys215, Val216, and Ala217 were less flexible upon the inhibition (Fig. S4). Consistently, Lys215 was identified to form a hydrogen bond with Glu31 from BLIP in the crystal

3

structure.[9,17] This hydrogen bond stabilizes the whole loop and could account for the decreased exchange rate. Besides, Val216 contacts with Asp49 and Tyr50 in BLIP through van der Waals interactions, thus becoming less flexible after the binding. Since Ala217 has no contacts with any residues from BLIP, the protection of this residue is probably due to the conformational change induced by the neighborhood. In contrast to our results, the crystal structure of the TEM1-BLIP complex (PDB ID: 1jtg) showed that TEM1 residues 214-217 (within the H10 region) are disordered compared to that of TEM1 (PDB ID: 1btl). We further investigated two newer crystal structures of TEM1 with BLIP-Y51A (PDB ID: 3c7u) and BLIP-Y150A (PDB ID: 3c7v). They both showed relatively low B-factors (Fig. S5) and excellent electron densities in the H10 region.[17] The disorder observed in the TEM1-BLIP complex (PDB ID: 1jtg) was therefore more likely to be an experimental artefact under that particular crystallization conditions. Compared to B-factor that indicates protein dynamics in crystal state,[34] HDX-MS used in this study reflects protein dynamics in solution state and thus can reveal dynamics information that might not be obtained by using B-factors.

Another considerable difference was shown for residues 230-246, which covers the β7-β8 loop adjacent to the H10 region. This motif comprises part of the active cavity that interacts with the β-hairpin loop in BLIP. Three residues on this motif, i.e., Lys234, Ser235 and Arg243, forms essential hydrogen bonds with Asp49 in BLIP,[9] thus these residues could be more protected from deuterium exchange. Interestingly, we identified residues 170-177 (C-terminus of Ω loop), which showed slower exchange after formation of the complex, but there was no hydrogen bond formed in this region. This helical loop is quite flexible in the free state and is more rigid in the bound state as indicated by MD simulation (Fig. 7d). By comparison of the crystal structures of the free and the bound forms (PDB IDs: 1btl and 1jtg), it was found that the helix structure is extended in this loop after the binding, which would protect the amide hydrogen from exchange.

Regarding the catalytic sites (Ser70, Ser130, and Glu166), a fragment (residues 127-137) covering the SDN loop was found to show decreased HDX. The involvement of the Ser130 in this loop in the binding of substrate has been reported.[35] More importantly, hydrogen bonding between Ser130 (TEM1) and Asp49 (BLIP) indicated that the reduced flexibility of this loop could improve the inhibition potency of BLIP.[9] A fragment (residues 163-169) located at the N-terminus of end of the Ω loop covering Glu166 showed decreased HDX in 1 min, suggesting minor change in dynamics at this region. In contrast, several fragments (residues 58-71, 59-71, 60-71 and 60-72) covering Ser70 maintained low level of deuterium exchange upon binding, suggesting that this region was highly protected in both states of TEM1. The trajectory analysis of Ser70, Ser130 and Glu166 showed

results that were consistent to HDX profiles of fragments covering these positions (Fig. S6, left panel).

Comparison of conformational changes among class A β-lactamases upon inhibition. Intriguingly, we detected an increased exchange at 10-min labelling for the N-terminus of protruding loop on both SHV1 and PC1 (Fig. 5), which could be partially involved in the binding interface from the point of view by crystallography.[13] Our result indicated that the residues 92-104, which comprise the N-terminus of the protruding loop close to the interface, became deprotected upon the binding. This strongly suggested that the conformational change of this loop occurred in an unfavorable manner for tight binding with BLIP. Such unfavored interactions lead to the loss of a salt-bridge between SHV1 (Asp104) or PC1 (Ala104) and BLIP (Lys74), which is preserved in the complex of TEM1 and BLIP. Furthermore, it has been demonstrated that the single mutation of SHV1 (D104E) and PC1 (A104E) would significantly enhance the binding affinity with BLIP,[5,18] highlighting the important role of residue at position 104 for effective inhibition. As mentioned before, this loop in TEM1 is more rigid than that in SHV1 and PC1. The conformational dynamics of this loop could be crucial to the inhibitory binding, indicating that rigid and convex shape of this loop in class A β-lactamase could dock better onto the concave interface in BLIP. Assumably, the preference of rigid interface reduced the entropic penalty of unfavorable conformational change, thus enhancing the inhibitory binding.

H10 region in SHV1 (211-225) and PC1 (211-228) showed the most significantly decreased deuterium exchange as observed in TEM1, indicating that this region was stabilized in all the inhibitory interactions under investigation (Figs. 4 & 5). Based on the crystal structures of SHV1 and BLIP complex (PDB IDs: 1shv and 2g2u), the H10 region was displaced to the core of active pocket in the complex.[13] Such conformational change was consistent with our observation. Besides, it has been reported that two novel inhibitors allosterically inactivated TEM1 through destabilization of the H10 region,[36] which was recently further proven to be an evolutionarily conserved allosteric site unique to class A β-lactamases.[37] Our results by HDX-MS revealed the conformational dynamics of this cryptic site among class A β-lactamases and the considerable changes induced by BLIP binding. A recent study on the dynamics of TEM1 upon substrate binding showed a similar HDX change in the H10 region during catalytic processes.[38] By contrast, our work involved study of different class A β-lactamases and the inhibitor protein, extending the observation to a broader and more general scope. From the 10-ns MD trajectory of these enzymes, H10 showed flapping motion to modulate the binding pocket. This strongly suggested that the flexibility of the H10 region could be determinant for the effective binding with BLIP. Higher flexibility of H10 on TEM1 might facilitate the insertion of BLIP into the binding pocket, causing higher binding affinity towards the inhibitor. Together, disrupting H10 region

4

could be an alternative strategy to inactivate the class A β-lactamases.

As one of the highly conserved loops in class A β-lactamases, the SDN loop has been proven to be important for the structural stability and function by site-directed mutagenesis.[34] After the inhibitory binding, residues 127-137 which refer to the SDN loop in SHV1 showed increased deuterium uptake at 1 min of exchange (Fig. 5). On the contrary, the SDN loop in TEM1 and PC1 showed both decreased exchange level at 1 and 10 min upon the inhibition. MD simulation of Ser130 showed that this region on SHV1 was more flexible after the binding while it was less flexible on TEM1 and PC1 (Fig. S6). Besides, no difference in deuterium exchange was found for the SDN loops of TEM1 and SHV1 in their free states (Fig. 3c). Comparison of the sequences spanning residues 127-137 of SHV1 (ITMSDNTAANL) with TEM1 (ITMSDNSAANL) indicated that only the residue at position 133, a threonine for TEM1 and a serine for SHV1, is different. Since threonine has a bulkier sidechain than serine, it is reasonable that after the binding the SDN loop of TEM1 could be less flexible than that of SHV1. Furthermore, according to the crystal models of TEM1 and SHV1 (PDB IDs: 1btl and 1shv), both Thr133 and Ser133 have contacts with residues Val103 and Ser106 located on the protruding loop. However, due to the orientation of the side chain at position 133, the distance of the contact towards Ser106 in TEM1 (2.7Å) is shorter than that in SHV1 (3.1Å), indicating that TEM1 has a tighter structure than SHV1 in this region. As a result, this region was less protected after the inhibitory binding for SHV1 while the protection was enhanced for TEM1. Perturbation of SDN loop could be important to suppress the activity of the class A β-lactamases.

Specifically, PC1 shares lower sequence and structural similarity with TEM1 and SHV1, and the crystal model of the complex PC1/BLIP has not been available yet. We constructed the complex by homology modeling (see details in Methods) and equilibrated the structure by MD simulation. Our HDX data showed that the binding with BLIP induced some unique changes in PC1 covering the catalytic sites, Ser70 and Lys73. Decreased deuterium exchange was observed in fragment 69-80. Together with the results from the MD simulation, we confirmed that the fluctuation of Ser70 was obviously reduced after binding with BLIP (Fig. S6).

Enhanced inhibition by BLIP mutants. To further explore the role of protruding loop on the binding interface, we introduced two mutations at E73 and K74 on BLIP, which specifically couple with the residues 104-106 upon binding with SHV1 and PC1, respectively.[9] Strikingly, the inhibition towards SHV1 and PC1 could be significantly enhanced with K_i at nanomolar level by the single mutation of E73M and K74G on BLIP, respectively.[4,5] Intriguingly, our results showed that BLIP$_{E73M}$ and BLIP$_{K74G}$ reversed the deprotection effect on the N-terminal of the protruding loop on SHV1 and PC1 caused by wild-type BLIP, indicating a more stabilized binding

interface of the complexes (Figs. 6b & c). The stabilization of the protruding loop could majorly contribute to the enhanced inhibition potency of BLIP mutants towards SHV1 and PC1 β-lactamases. Previous studies reported that single mutation on the protruding at position 104 could also enhance the binding affinity of SHV1 and PC1 towards wild-type BLIP.[4,5] Together, it can be concluded that the interactions between the protruding loop and BLIP is crucial for novel design of BLIP derived inhibitors.

BLIP$_{E73M}$ also eliminated the deprotection effect from wild-type BLIP towards the SDN region of SHV1, which could facilitate more effective inhibition (Fig. 6b). In contrast, BLIP$_{K74G}$ showed more protection of residues 50-79 in PC1 including active sites Ser70 and Lys73, which could severely inactivate the function of these sites (Fig. 6c). Both BLIP mutants demonstrated predominant protection in the H10 region of SHV1 and PC1, similarly reflected in the inhibition by the wild-type BLIP. Such conformational changes indicated a common mechanism of the bindings between these β-lactamases and BLIP as discussed above.

Tyr50 on BLIP forms favorable interactions with several key regions on β-lactamases, including Pro107 on protruding loop, Met129 on SDN region and Val216 on H10 region.[9] Strangely, alanine substitution of this residue can further promote the potency towards TEM1 with K_i at picomolar level.[39] Although the Ala50 would lose several contacts with TEM1, presumably it could eliminate the colliding effect caused by the side-chain of Tyr50 and allow a more favorable conformation of Asp49.[39] More significant protections from HDX were observed in SDN loop and β7-β8 in TEM1 upon inhibition by BLIP$_{Y50A}$ (Fig. 6a), suggesting more stabilized conformations of these regions. Our results could support that Asp49 might show a more favorable conformation, which interacted more intensively with SDN loop (Ser130) and β7-β8 (Lys233, Ser234 and Arg244) in the complex.[9] This might be the major cause for the enhanced inhibition of TEM1.

Interestingly, obvious deprotection of the N-terminal helix, which is far away from the active binding domain, indicated that relaxation of this region might be favorable in the cases of strong inhibition (Fig. 6a). A recent study showed that the mutation Q39K on the N-terminal helix of TEM1 destabilized the protein, revealing that interactions involved in this region could significantly influence the binding and catalytic properties of the protein.[41] Such observation, which might not be obtained by other techniques, could support that deprotection of this region might suppress the activity of β-lactamases.

MD simulation revealed protein dynamics at complementary time scale to HDX. Obviously, the deviation of TEM1 was reduced upon binding BLIP while it was maintained for SHV1 and PC1 (Figs. 7a-c). This result showed consistency with that obtained with global HDX (Figs. 3a). Our results confirmed that the global stabilization of TEM1 upon binding was more obvious than

that of the others during the period of simulation. It should be noted that the simulation was examined at ns time scale, and thus it might not necessarily be consistent but complementary to some HDX results that reflected protein dynamics at μs to ms scale.[42] However, integration of these two techniques enabled us to dig into some unique dynamic features of the proteins.

The last 5-ns simulation showed that most regions across these β-lactamases had similar fluctuations, strongly indicating similar folding of the proteins. Interestingly, variation was found in the Ω loop, where TEM1 showed the much higher fluctuation than PC1 and SHV1 (Fig. 7g). This result was complementary to the result obtained by HDX-MS, which showed that this loop in PC1 was more flexible than that in TEM1 and SHV1 (Fig. 3c). This might be explained by the different timescales of the loop motion reflected by the MD simulation and HDX. A previous study by NMR demonstrated that the Ω loop of TEM1 was highly ordered on the ps-to-ns time scale while slow motions were observed on the μs-to-ms time scale,[19,20] supporting our assumption. Such dynamic duality plays an important role in the substrate binding and catalytic reaction. Taking advantage of our results from MD simulation and HDX-MS, we infer that the fast motion of Ω loop on TEM1 is faster than that on SHV1 and PC1, and in contrast, the slow motion of this loop on PC1 is faster than that on TEM1 and SHV1.

More interestingly, significant protection from HDX was detected in the C-terminus of Ω loop on all these class A β-lactamases after bound with BLIP (Figs. 4 & 5), indicating that the slow motion of this loop was suppressed. By contrast, the fluctuation of this loop was escalated on SHV1 and PC1 while it was attenuated on TEM1 (Figs. 7d-f). This observation suggested that the loop might be catalytically more active on SHV1 and PC1 than on TEM1 upon bound with BLIP. Such difference could explain the lower inhibition potency of BLIP towards SHV1 and PC1. Together, it was strongly suggested that the motion of Ω loop was affected in both fast and slow fashions upon the inhibition.

Conclusions

Although class A β-lactamases are highly similar with respect to their sequences and structures, our results revealed that SHV1 exhibited the most compact conformation, while PC1 was most extended. After inhibition by BLIP, TEM1 was globally more rigid while SHV1 and PC1 showed no significant change in conformational dynamics. The protruding loop on TEM1 showed remarkable change in conformational dynamics upon BLIP binding. However, the N-terminus of the protruding loop on SHV1 and PC1 were both deprotected from HDX upon the binding, indicating the unfavorable interactions in this region. BLIP mutants, BLIP$_{E73M}$ and BLIP$_{K74G}$, reversed this deprotecting effects on SHV1 and PC1 and stabilized the interfaces of these bindings. Rigid conformation of this interface might be favored to reduce the entropic penalty of the binding. Unexpectedly, marked conformational changes in the H10 region were observed upon the inhibition. Although this region is far away from the binding interface, it could modulate the plasticity of the binding pocket and enhance the inhibition of the enzymes. Conformational dynamics of several functional loops, i.e., SDN loop, β7-β8 loop and Ω loop, provided novel and unique insights into the mechanistic process of these inhibitory interactions. Cooperative interaction of these loops with BLIP could improve the inhibition potency of BLIP towards the class A β-lactamases.

Potent inhibitors such as engineered BLIPs can be rationally designed to bind β-lactamases by disrupting the flexibility of the loop regions, especially H10 region and SDN loop. To conclude, our study is the first to provide comprehensive insights into the conformational dynamics of class A β-lactamases upon inhibitory binding with BLIP, which implies alternative and unique strategies for the study of β-lactamases and the design of novel inhibitors.

Experimental

The proteins were expressed, purified and characterized as described in the Supporting Information. Native MS, IM-MS and HDX-MS were performed using a Synapt G2 Si mass spectrometer (Waters, UK). Experimental details can be found in the Supporting Information.

ASSOCIATED CONTENT

Supporting Information

Materials and Methods; Table S1; Figures S1-S7.

AUTHOR INFORMATION

Corresponding Author

Zhong-Ping Yao
Department of Applied Biology and Chemical Technology
The Hong Kong Polytechnic University
Hung Hom, Kowloon
Hong Kong
Email: zhongping.yao@polyu.edu.hk

REFERENCES

(1) Dawz, S.; Bonomo, R. A. Three Decades of β-Lactamase Inhibitors. Clin. Microbiol. Rev. 2010, 23 (1), 160–201. https://doi.org/10.1128/cmr.00037-09.

(2) Philippon, A.; Slama, P.; Dény, P.; Labia, R. A Structure-Based Classification of Class A β-Lactamases, a Broadly Diverse Family of Enzymes. Clin. Microbiol. Rev. 2016, 29 (1), 29–57. https://doi.org/10.1128/CMR.00019-15.

(3) Bush, K.; Jacoby, G. A. Updated Functional Classification of β-Lactamases. Antimicrob. Agents. Ch. 2010, 54 (3), 969–976. https://doi.org/10.1128/AAC.01009-09.

(4) Reynolds, K. A.; Hanes, M. S.; Thomson, J. M.; Antczak, A. J.; Berger, J. M.; Bonomo, R. A.; Kirsch, J. F.; Handel, T. M. Computational Redesign of the SHV-1 β-Lactamase/β-Lactamase Inhibitor Protein Interface. J. Mol. Biol. 2008, 382 (5), 1265–1275. https://doi.org/10.1016/j.jmb.2008.05.051.

(5) Yuan, J.; Chow, D.-C.; Huang, W.; Palzkill, T. Identification of a β-Lactamase Inhibitory Protein Variant That Is a Potent Inhibitor of Staphylococcus PC1 β-Lactamase. J. Mol. Biol. 2011, 406 (5), 730–744. https://doi.org/10.1016/j.jmb.2011.01.014.

(6) Jelsch, C.; Mourey, L.; Masson, J.; Samama, J. Crystal Structure of Escherichia Coli TEM1 B-lactamase at 1.8 Å Resolution. Proteins 1993, 16 (4), 364–383. https://doi.org/10.1002/prot.340160406.

(7) Kuzin, A. P.; Nukaga, M.; Nukaga, Y.; Hujer, A. M.; Bonomo, R. A.; Knox, J. R. Structure of the SHV-1 β-Lactamase†. Biochemistry 1999, 38 (18), 5720–5727. https://doi.org/10.1021/bi990136d.

(8) Herzberg, O. Refined Crystal Structure of β-Lactamase from Staphylococcus Aureus PC1 at 2.0 Å Resolution. J. Mol. Biol. 1991, 217 (4), 701–719. https://doi.org/10.1016/0022-2836(91)90527-D.

(9) Strynadka, N. C. J.; Jensen, S. E.; Alzari, P. M.; James, M. N. G. A Potent New Mode of β-Lactamase Inhibition Revealed by the 1.7 Å X-Ray Crystallographic Structure of the TEM-1–BLIP Complex. Nat Struct Mol Biol 1996, 3 (3), 290–297. https://doi.org/10.1038/nsb0396-290.

(10) Strynadka, N.; Jensen, S. E.; Johns, K.; Blanchard, H.; Page, M.; Matagne, A.; Frère, J.-M.; James, M. Structural and Kinetic Characterization of a β-Lactamase-Inhibitor Protein. Nature 1994, 368 (6472), 657–660. https://doi.org/10.1038/368657a0.

(11) Gretes, M.; Lim, D. C.; de Castro, L.; Jensen, S. E.; Kang, S. G.; Lee, K. J.; Strynadka, N. C. Insights into Positive and Negative Requirements for Protein-Protein Interactions by Crystallographic Analysis of the Beta-Lactamase Inhibitory Proteins BLIP, BLIP-I, and BLP. J. Mol. Biol. 2009, 389 (2), 289–305. https://doi.org/10.1016/j.jmb.2009.03.058.

(12) Brown, N. G.; Chow, D.-C.; Sankaran, B.; Zwart, P.; Prasad, V. B.; Palzkill, T. Analysis of the Binding Forces Driving the Tight Interactions between β-Lactamase Inhibitory Protein-II (BLIP-II) and Class A β-Lactamases. J. Biol. Chem. 2011, 286 (37), 32723–32735. https://doi.org/10.1074/jbc.m111.265058.

(13) Reynolds, K. A.; Thomson, J. M.; Corbett, K. D.; Bethel, C. R.; Berger, J. M.; Kirsch, J. F.; Bonomo, R. A.; Handel, T. M. Structural and Computational Characterization of the SHV-1 β-Lactamase-β-Lactamase Inhibitor Protein Interface. J. Biol. Chem. 2006, 281 (36), 26745–26753. https://doi.org/10.1074/jbc.m603878200.

(14) Reichmann, D.; Rahat, O.; Albeck, S.; Meged, R.; Dym, O.; Schreiber, G. The Modular Architecture of Protein–Protein Binding Interfaces. Proc. Natl. Acad. Sci. U.S.A. 2005, 102 (1), 57–62. https://doi.org/10.1073/pnas.0407280102.

(15) Cohen-Khait, R.; Schreiber, G. Low-Stringency Selection of TEM1 for BLIP Shows Interface Plasticity and Selection for Faster Binders. Proc. Natl. Acad. Sci. U.S.A. 2016, 113 (52), 14982–14987. https://doi.org/10.1073/pnas.1613122113.

(16) Rudgers, G. W.; Palzkill, T. Identification of Residues in β-Lactamase Critical for Binding β-Lactamase Inhibitory Protein.

J. Biol. Chem. 1999, 274 (11), 6963–6971. https://doi.org/10.1074/jbc.274.11.6963.

(17) Wang, J.; Palzkill, T.; Chow, D.-C. Structural Insight into the Kinetics and ΔCp of Interactions between TEM-1 β-Lactamase and β-Lactamase Inhibitory Protein (BLIP). J. Biol. Chem. 2009, 284 (1), 595–609. https://doi.org/10.1074/jbc.M804089200.

(18) Hanes, M. S.; Reynolds, K. A.; McNamara, C.; Ghosh, P.; Bonomo, R. A.; Kirsch, J. F.; Handel, T. M. Specificity and Cooperativity at B-lactamase Position 104 in TEM-1/BLIP and SHV-1/BLIP Interactions. Proteins 2011, 79 (4), 1267–1276. https://doi.org/10.1002/prot.22961.

(19) Savard, P.-Y.; Gagné, S. M. Backbone Dynamics of TEM-1 Determined by NMR: Evidence for a Highly Ordered Protein†. Biochemistry-us 2006, 45 (38), 11414–11424. https://doi.org/10.1021/bi060414q.

(20) Fisette, O.; Morin, S.; Savard, P.-Y.; Lagüe, P.; Gagné, S. M. TEM-1 Backbone Dynamics—Insights from Combined Molecular Dynamics and Nuclear Magnetic Resonance. Biophys J 2010, 98 (4), 637–645. https://doi.org/10.1016/j.bpj.2009.08.061.

(21) Uetrecht, C.; Rose, R. J.; van Duijn, E.; Lorenzen, K.; Heck, A. J. Ion Mobility Mass Spectrometry of Proteins and Protein Assemblies. Chem. Soc. Rev. 2009, 39 (5), 1633–1655. https://doi.org/10.1039/b914002f.

(22) Zhang, Z.; Smith, D. L. Determination of Amide Hydrogen Exchange by Mass Spectrometry: A New Tool for Protein Structure Elucidation. Protein Sci. 1993, 2 (4), 522–531. https://doi.org/10.1002/pro.5560020404.

(23) Yao, Z.; Zhou, M.; Kelly, S. E.; Seeliger, M. A.; Robinson, C. V.; Itzhaki, L. S. Activation of Ubiquitin Ligase SCFSkp2 by Cks1: Insights from Hydrogen Exchange Mass Spectrometry. J. Mol. Biol. 2006, 363 (3), 673–686. https://doi.org/10.1016/j.jmb.2006.08.032.

(24) Skinner, J. J.; Lim, W. K.; Bédard, S.; Black, B. E.; Englander, W. S. Protein Dynamics Viewed by Hydrogen Exchange. Protein Sci. 2012, 21 (7), 996–1005. https://doi.org/10.1002/pro.2081.

(25) Marcsisin, S. R.; Engen, J. R. Hydrogen Exchange Mass Spectrometry: What Is It and What Can It Tell Us? Anal. Bioanal. Chem. 2010, 397 (3), 967–972. https://doi.org/10.1007/s00216-010-3556-4.

(26) Karplus, M.; Kuriyan, J. Molecular Dynamics and Protein Function. Proc. Natl. Acad. Sci. U.S.A. 2005, 102 (19), 6679–6685. https://doi.org/10.1073/pnas.0408930102.

(27) Huang, L. W.; So, P. K.; Yao, Z. P. Protein Dynamics Revealed by Hydrogen/Deuterium Exchange Mass Spectrometry: Correlation between Experiments and Simulation. Rapid Commun. Mass Spectrom. 2019. 33 (S3), 83-89. https://doi.org/10.1002/rcm.8307.

(28) Zhu, S.; Khatun, R.; Lento, C.; Sheng, Y.; Wilson, D. J. Enhanced Binding Affinity via Destabilization of the Unbound State: A Millisecond Hydrogen–Deuterium Exchange Study of the Interaction between P53 and a Pleckstrin Homology Domain. Biochemistry-us 2017, 56 (32), 4127–4133. https://doi.org/10.1021/acs.biochem.7b00193.

(29) Chetty, P. S.; Mayne, L.; Lund-Katz, S.; Englander, W. S.; Phillips, M. C. Helical Structure, Stability, and Dynamics in Human Apolipoprotein E3 and E4 by Hydrogen Exchange and Mass Spectrometry. Proc. Natl. Acad. Sci. USA 2017, 114 (5), 968–973. https://doi.org/10.1073/pnas.1617523114.

(30) Banerjee, S.; Pieper, U.; Kapadia, G.; Pannell, L. K.; Herzberg, O. Role of the Ω-Loop in the Activity, Substrate Specificity, and Structure of Class A β-Lactamase. Biochemistry-us 1998, 37 (10), 3286–3296. https://doi.org/10.1021/bi972127f.

(31) Stojanoski, V.; Chow, D.-C.; Hu, L.; Sankaran, B.; Gilbert, H. F.; Prasad, V. B.; Palzkill, T. A Triple Mutant in the Ω-Loop of

TEM-1 β-Lactamase Changes the Substrate Profile via a Large Conformational Change and an Altered General Base for Catalysis. J. Biol. Chem. 2015, 290 (16), 10382–10394. https://doi.org/10.1074/jbc.m114.633438.

(32) Hamuro, Y.; Zhang, T. High-Resolution HDX-MS of Cytochrome c Using Pepsin/Fungal Protease Type XIII Mixed Bed Column. J. Am. Soc. Mass Spectrom. 2019, 30 (2), 227–234. https://doi.org/10.1007/s13361-018-2087-7.

(33) Li, M.; Conklin, B. C.; Taracila, M. A.; Hutton, R. A.; Skalweit, M. J. Substitutions at Position 105 in SHV Family β-Lactamases Decrease Catalytic Efficiency and Cause Inhibitor Resistance. Antimicrob. Agents. Ch. 2012, 56 (11), 5678–5686. https://doi.org/10.1128/AAC.00711-12.

(34) Liu, Q.; Li, Z.; Li, J. Use B-Factor Related Features for Accurate Classification between Protein Binding Interfaces and Crystal Packing Contacts. Bmc Bioinformatics 2014, 15 Suppl 16 (S16), S3. https://doi.org/10.1186/1471-2105-15-s16-s3.

(35) Jacob, F.; Joris, B.; Lepage, S.; Dusart, J.; Frère, J. Role of the Conserved Amino Acids of the 'SDN' Loop (Ser130, Asp131 and Asn132) in a Class A β-Lactamase Studied by Site-Directed Mutagenesis. Biochem. J. 1990, 271 (2), 399–406. https://doi.org/10.1042/bj2710399.

(36) Horn, J. R.; Shoichet, B. K. Allosteric Inhibition Through Core Disruption. J. Mol. Biol. 2004, 336 (5), 1283–1291. https://doi.org/10.1016/j.jmb.2003.12.068.

(37) Avci, F.; Altinisik, F.; Ulu, D.; Olmez, E.; Akbulut, B. An Evolutionarily Conserved Allosteric Site Modulates Beta-Lactamase Activity. J. Enzyme. Inhib. Med. Chem. 2016, 31(S3), 33-40. https://doi.org/10.1080/14756366.2016.1201813.

(38) Knox, R., Lento, C., Wilson, D. Mapping Conformational Dynamics to Individual Steps in the TEM-1 β-Lactamase Catalytic Mechanism J. Mol. Biol. 2018, 430 (18), 3311-3322. https://dx.doi.org/10.1016/j.jmb.2018.06.045

(39) Zhang, Z., Palzkill, T. Determinants of Binding Affinity and Specificity for the Interaction of TEM-1 and SME-1 β-Lactamase with β-Lactamase Inhibitory Protein. J. Biol. Chem. 2003, 278(46), 45706–45712. https://dx.doi.org/10.1074/jbc.m308572200.

(40) Wang, J., Zhang, Z., Palzkill, T., Chow, D. Thermodynamic Investigation of the Role of Contact Residues of β-Lactamase-inhibitory Protein for Binding to TEM-1 β-Lactamase. J. Biol. Chem. 2007, 282(24), 17676-17684. https://dx.doi.org/10.1074/jbc.m611548200.

(41) Shcherbinin, D., Rubtsova, M., Grigorenko, V., Uporov, I., Veselovsky, A., Egorov, A. The study of the role of mutations M182T and Q39K in the TEM-72 β-lactamase structure by the molecular dynamics method. Biochemistry (Moscow) 2017, 11(2), 120-127. https://doi.org/10.1134/S1990750817020056.

(42) McAllister, R., Konermann, L. Challenges in the interpretation of protein h/d exchange data: a molecular dynamics simulation perspective. Biochemistry-us 2015, 54(16) 2683-2692. https://dx.doi.org/10.1021/acs.biochem.5b00215.

Figure captions

Fig. 1 β-Lactamases and their complexes with BLIP. (a) Sequence alignment of TEM1, SHV1 and PC1. Regions of helix and sheet are labelled. **(b)** Representative model of the complex of β-lactamases (i.e., TEM1) and BLIP (PDB ID: 1JTG). Loops of interest are labelled on TEM1. **(c)** Characteristic properties of TEM1, SHV1 and PC1. The values of inhibition constants and sequence identity are obtained from literatures.[4,5,38] Structures of TEM1 (PDB IDs: 1btl and 1jtg), SHV1 (PDB IDs: 1shv and 2g2u) and PC1 (PDB ID: 3blm) are superimposed using PyMOL.

Fig. 2 Native MS and IM-MS results for the interactions between β-lactamases and BLIP. (a) Native mass spectra of β-lactamases in their free (hollow) and BLIP-bound (filled) states. **(b)** Arrival time distribution of SHV1, PC1 and TEM1 in their free states (left panel) and BLIP bound states (right panel). Charge states at 10+ in the free states and charge states at 14+ in the bound states were presented.

Fig. 3 HDX-MS results for free β-lactamases. (a) Global deuterium uptake plots of β-lactamases in their free (left) and BLIP bound (right) states. **(b)** Fractional deuterium uptake at 1 and 10 min is mapped onto the crystal models of TEM1 (PDB ID: 1btl), SHV1 (PDB ID: 1shv) and PC1 (PDB ID: 3blm). Deuterium uptake is labelled as the color bar indicated. **(c)** Fractional deuterium uptake of H10 region, SDN loop, N-terminal Protruding loop and C-terminal Ω-loop from TEM1 (blue), SHV1 (orange) and PC1 (red) were compared at 1- and 10-min labelling.

Fig. 4 HDX-MS results for TEM1/BLIP interaction. (a) HDX difference (ΔHDX) for all identified peptides from TEM1. Key secondary structures are shown on the top. Error bars indicate standard deviations at 1 and 10 min (n=3, significant ΔHDX > 0.29 Da). **(b)** Summed fractional HDX difference of 1- and 10-min labelling was labelled onto the crystal model of TEM1 (PDB ID: 1BTL). Active sites are shown as yellow stick.

Fig. 5 HDX-MS results for SHV1/BLIP and PC1/BLIP interactions. (a) HDX difference for all identified peptides from SHV1 with significant ΔHDX > 0.26 Da. **(b)** HDX difference for all identified peptides from PC1 with significant ΔHDX > 0.46 Da. Error bars indicate standard deviations for the time points 1 and 10 min (n=3). Summed fractional HDX difference of 1- and 10-min labelling was labelled onto the crystal model of **(c)** SHV1 and **(d)** PC1 in HDX after binding with BLIP.

Fig. 6 HDX-MS results for the interactions between β-lactamases and BLIP mutants. (a)-(c) HDX difference for peptides from TEM1 (significant ΔHDX > 0.21 Da), SHV1 (significant ΔHDX > 0.24 Da) and PC1 (significant ΔHDX > 0.55 Da) were plotted. Error bars indicate standard deviations for the time points 1 and 10 min (n=3). **(d)-(f)** Summed fractional HDX differences of 1- and 10-min labelling were labelled onto the crystal models of TEM1 (PDB ID: 1BTL), SHV1 (PDB ID: 1SHV) and PC1 (PDB ID: 3BLM) on the right panel.

Fig. 7 10-ns molecular dynamics simulation of β-lactamases upon binding BLIP. (a)-(c) Root mean square deviation (RMSD) as a function of time (ns) for the free (blue) and BLIP-bound (orange) TEM1, SHV1 and PC1 β-lactamases. **(d)-(f)** Differences in root mean square fluctuation (RMSF) of individual residue upon BLIP binding during 5-10 ns simulation were mapped onto the crystal models of TEM1, SHV1 and PC1. **(g)** RMSF of the β-lactamases is plotted against individual residue.

a

α1-β1 loop   **β2-α2 loop**

```
TEM1  --MHPETLVKVKDAEDQLGARVGYIELDLNSGKILESFRPEERFPMMSTFKVLLCGAVLS
SHV1  --MSPQPLEQIKLSESQLSGRVGMIEMDLASGRTLTAWRADERFPMMSTFKVVLCGAVLA
PC1   MHHHHHHMKELNDLEKKYNAHIGVYALDTKSGKEV-KFNSDKRFAYASTSKAINSAILLE
         .   : .   :   :   **:  . ** :: **** .*  **  *
```

Protruding loop   **SDN loop**

```
TEM1  RVDAGQEQLGRRIHYSQNDLVEYSPVTEKHLTDGMTVRELCSAAITMSDNTAANLLLTTI
SHV1  RVDAGDEQLERKIHYRQQDLVDYSPVSEKHLADGMTVGELCAAAITMSDNSAANLLLATV
PC1   QVP--YNKLNKKVHINKDDIVAYSPILEKYVGKDITLKALIEASMTYSDNTANNKIIKEI
       :*    ::: ::::   :*.***: **:  . *** ***:.* *    :
```

Omega-loop

```
TEM1  GGPKELTAFLHNMGDHVTRLDRWEPELNEAIPNDERDTTMPAAMATTLRKLLTGELLTLA
SHV1  GGPAGLTAFLRQIGDNVTRLDRWETELNEALPGDARDTTTPASMAATLRKLLTSQRLSAR
PC1   GGIKKVKQRLKELGDKVTNPVRYEIELNYYSPKSKKDTSTPAAFGKTLNKLIANGKLSKE
      **   .  :* : **:**  .*:* :***    .  :* :**:   .* :*: ..   *
```

Helix10 region   **β7-β8 loop**

```
TEM1  SRQQLIDWMEADKVAGPLLRSALPAGWFIADKSGAGE-RGSRGIIAALGPDGKPSRIVVI
SHV1  SQRQLLQWMVDDRVAGPLIRSVLPAGWFIADKTGAGE-RGARGIVALLGPNNKAERIVVI
PC1   NKKFLLDLMLNNKSGDTLIKDGVPKDYKVADKSGQAITYASRNDVAFVYPKGQSEPIVLV
      .:  * .:* .     . :   .* .:   ***:* :  .:*  ::  : .*. . *::
```

β9-α12 loop

```
TEM1  YTTGSQATMDER-NRQIAEIGASLIKHWSHHHHHH-
SHV1  YLRDTPASMAER-NQQIAGIGAALIEHWQRHHHHHH
PC1   IFTNKDNKSDKPNDKLISETAKSVMKEF--------
      : . . ::    .   .  * :* :** : :::::
```

Legend:
- **Helix** (blue oval)
- **Strand** (orange arrow)

b

α1-β1 loop | **β9-α12 loop** | **Omega-loop** | **Protruding loop** | **β7-β8 loop** | **Helix10 region** | **β2-α2 loop** | **SDN loop**

BLIP   180°   BLIP

c

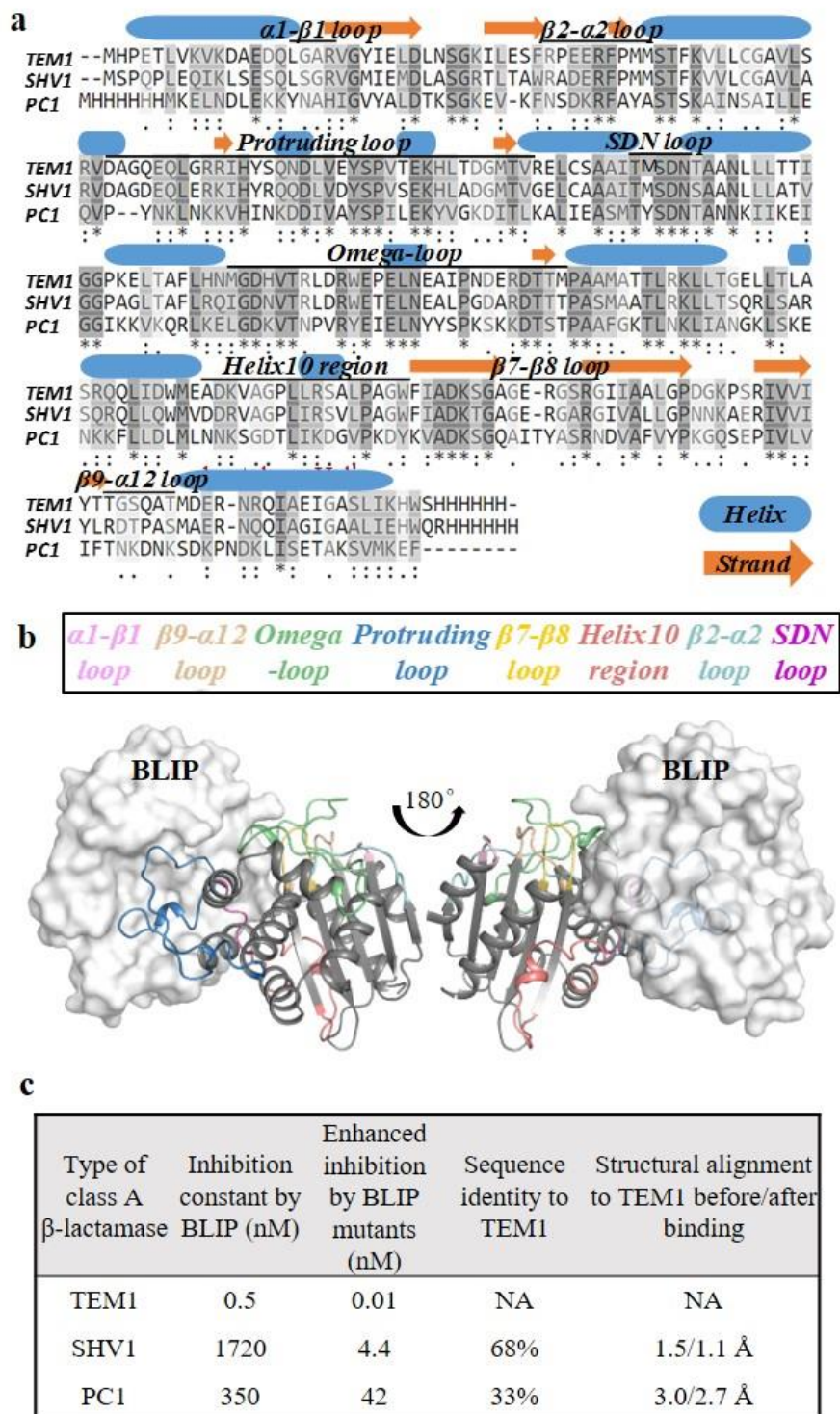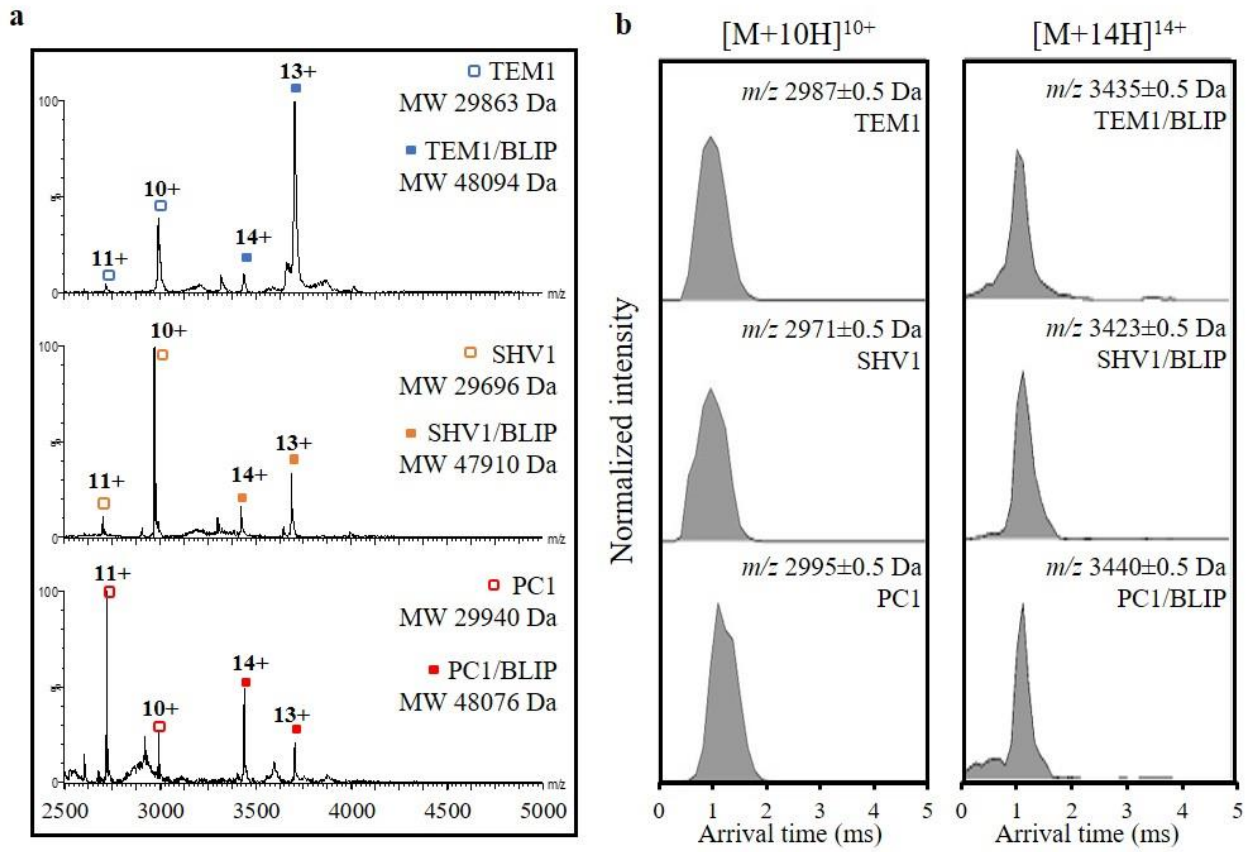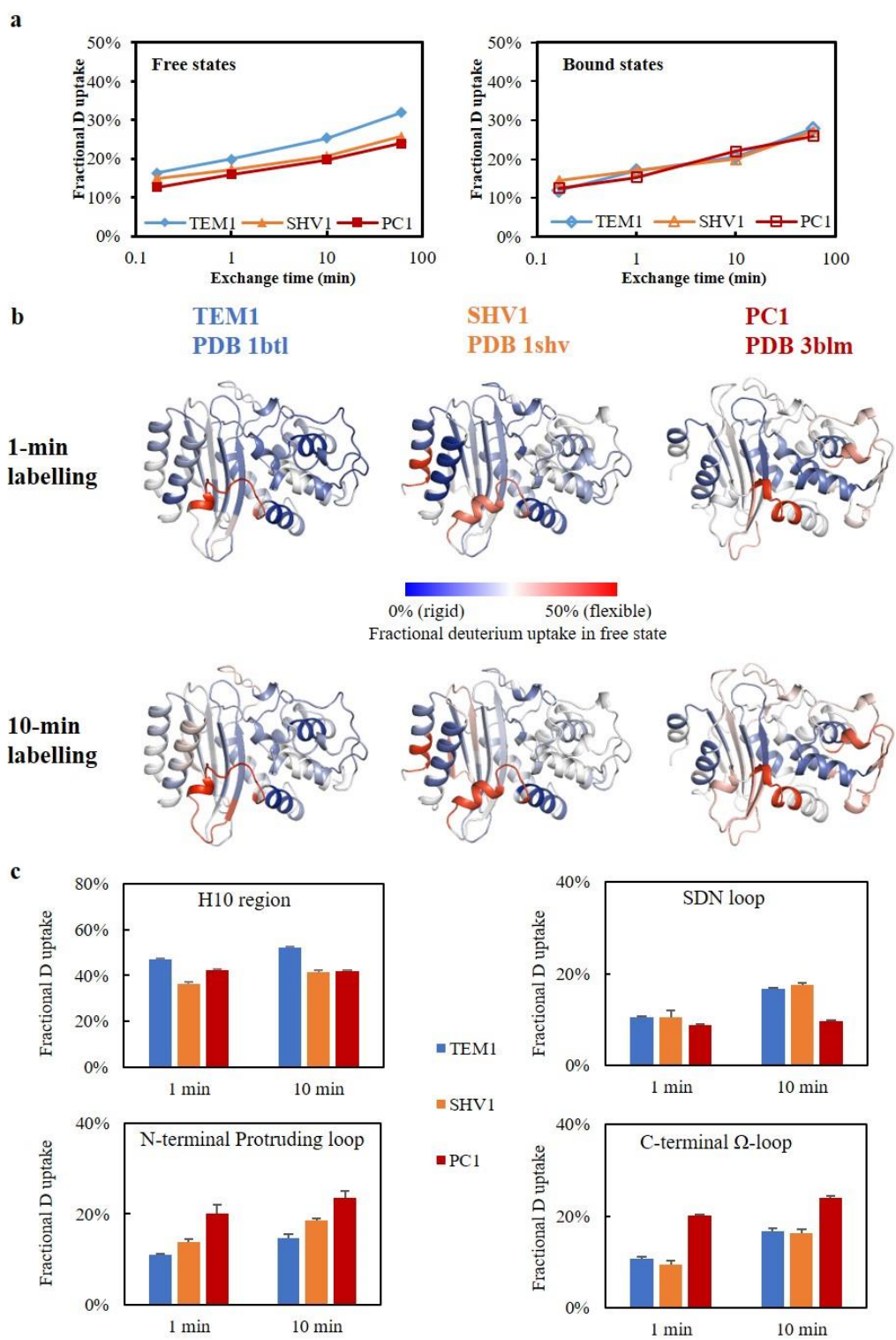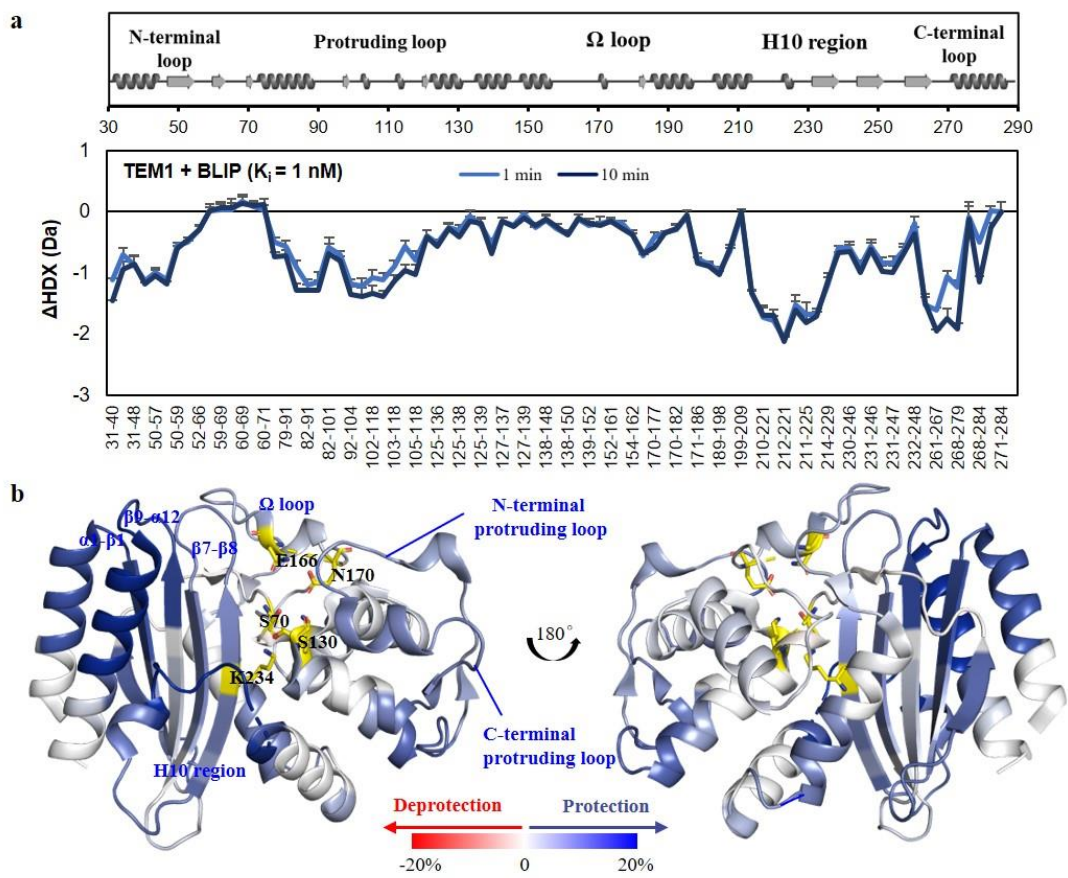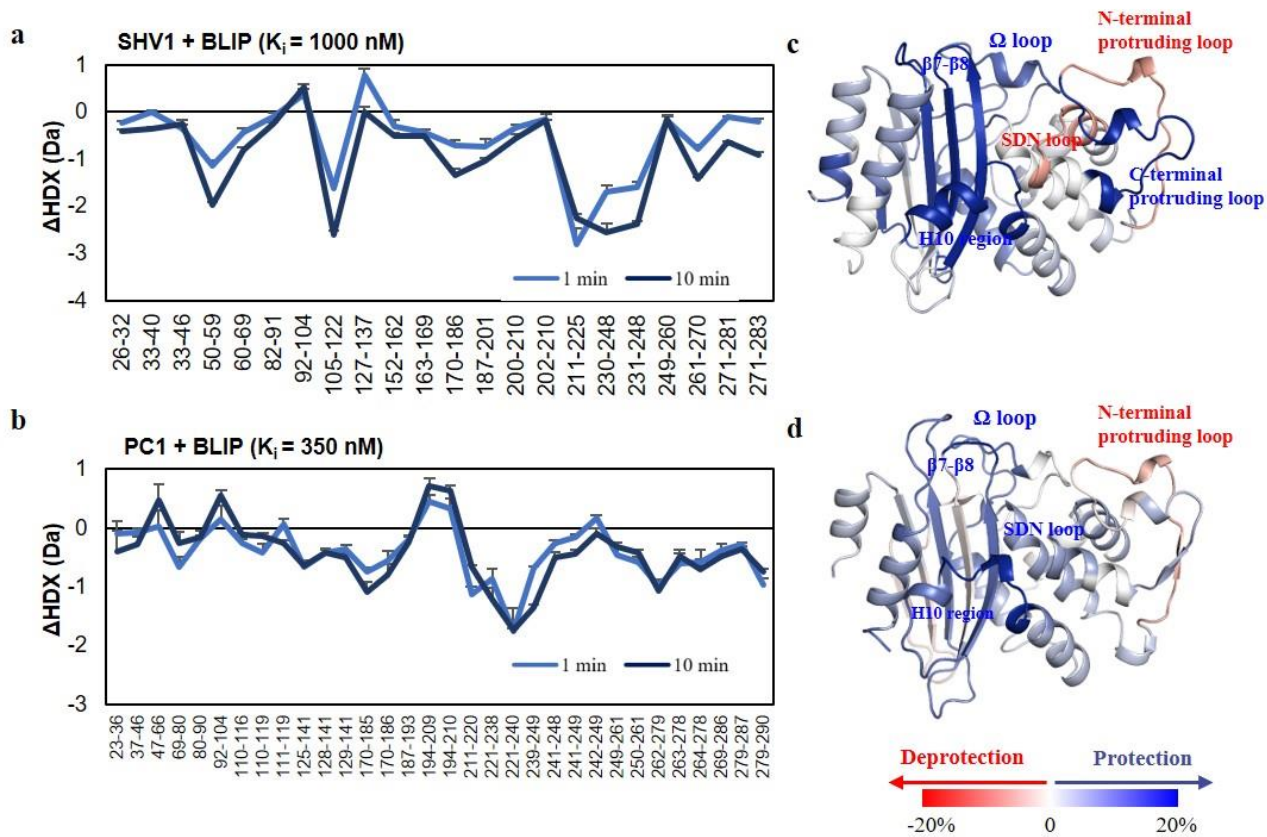| Type of class A β-lactamase	Inhibition constant by BLIP (nM)	Enhanced inhibition by BLIP mutants (nM)	Sequence identity to TEM1	Structural alignment to TEM1 before/after binding
TEM1	0.5	0.01	NA	NA
SHV1	1720	4.4	68%	1.5/1.1 Å
PC1	350	42	33%	3.0/2.7 Å

Figure 1

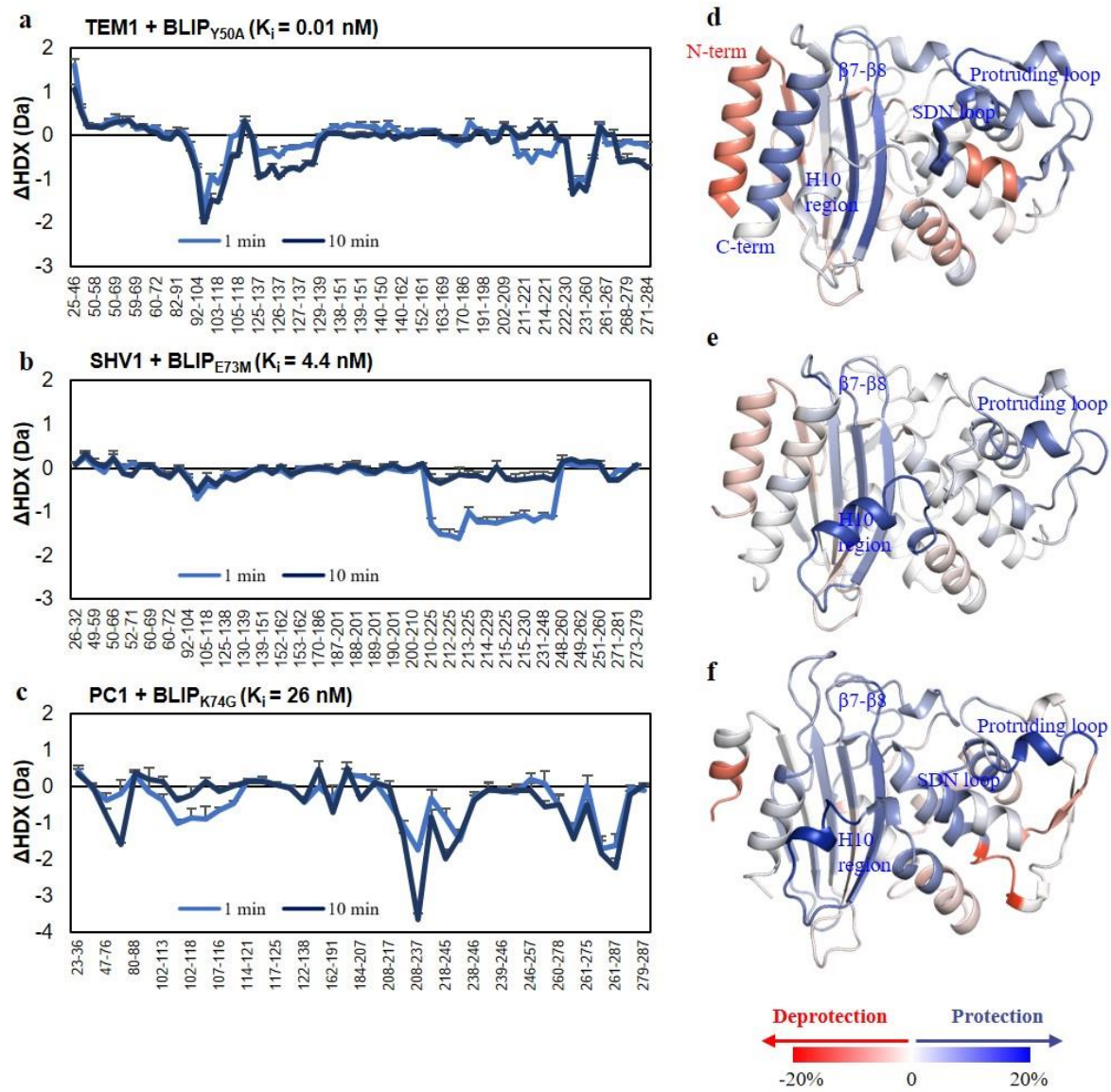Figure 2

Figure 3
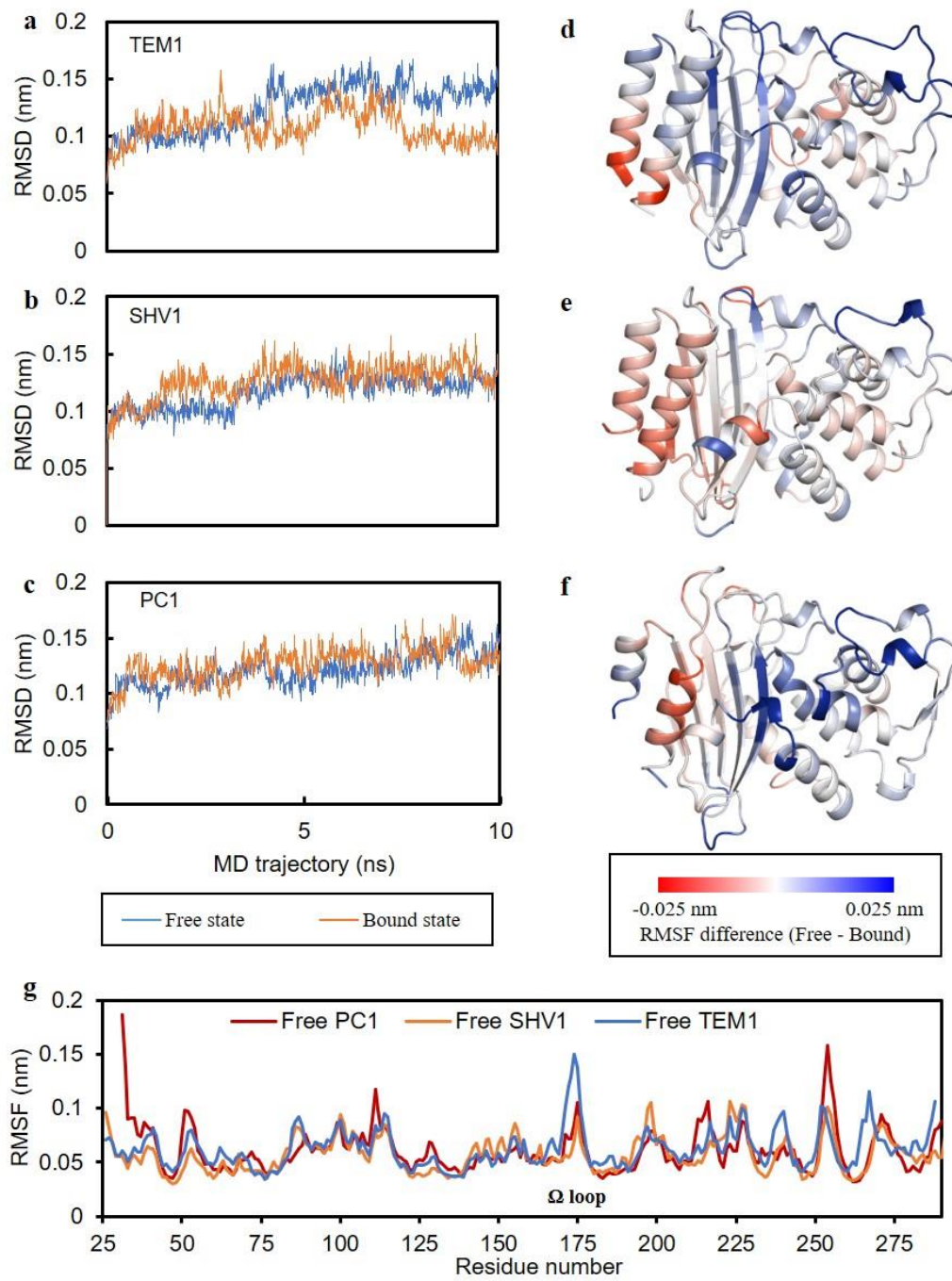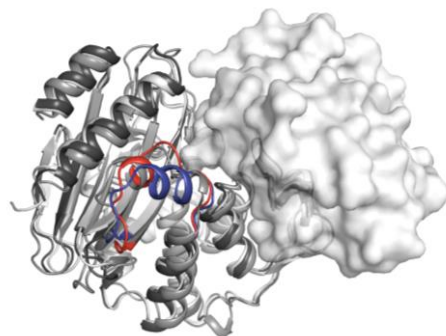
Figure 4

Figure 5

Figure 6

Figure 7

TOC only

Helix 10 region as allosteric site

Supporting Information

Conformational Dynamics of Helix 10 Region as An Allosteric Site in Class A β-Lactamase Inhibitory Binding

Liwen Huang[1], Pui-Kin So[1], Yu Wai Chen[1], Yun-Chung Leung[1], Zhong-Ping Yao[1,2*]

[1]State Key Laboratory of Chemical Biology and Drug Discovery, Food Safety and Technology Research Centre and Department of Applied Biology and Chemical Technology, The Hong Kong Polytechnic University, Hung Hom, Kowloon, Hong Kong Special Administrative Region, China

[2]State Key Laboratory of Chinese Medicine and Molecular Pharmacology (Incubation) and Shenzhen Key Laboratory of Food Biological Safety Control, Shenzhen Research Institute of The Hong Kong Polytechnic University, Shenzhen 518057, China

* Corresponding Author:

Zhong-Ping Yao

Department of Applied Biology and Chemical Technology

The Hong Kong Polytechnic University

Hung Hom, Kowloon

Hong Kong

Email: zhongping.yao@polyu.edu.hk

Contents:

Materials and Methods

Table S1

Figures S1-S7

Materials and Methods

Protein expression, purification and characterization. His-tagged TEM1, SHV1 and PC1 were expressed in E. coli BL21 (DE3) through modified plasmids containing the kanamycin-resistant gene, as previously described.[1] Briefly, transformed E. coli BL21 was cultured in Luria Broth containing kanamycin. Protein overexpression was induced with isopropyl β-D-1thiogalactopyranoside (IPTG) when OD_{600} of the culture reached 0.8. The bacteria were harvested by centrifugation at 4 °C followed by resuspension in lysis buffer (50 mM phosphate buffer, pH 7.4). Suspensions were lysed with sonication for 5 min at 15-sec intervals and insoluble debris was removed by centrifugation. The supernatant was filtered through a 0.45 μm filter and applied to a HisTrap[TM] HP affinity column (GE Healthcare) with 5 ml precharged Ni for purification. The purified proteins were buffer exchanged into 50 mM phosphate buffer. Their concentrations were determined by Bradford assay and NanoDrop (Thermo Fisher Scientific). Their molecular weights and purities were characterized by SDS-PAGE and MS. The enzyme activity was measured by the rate of degradation of nitrocefin, whose absorbance at 486 nm appears upon catalysis by β-lactamases. The initial slope of the reaction at steady state was determined using 2-10 nM enzyme and 200 μM nitrocefin. Reaction rates were plotted as a function of substrate concentration. The data were fitted to the Michaelis-Menten equation to determine k_{cat} and K_m. BLIP was produced following the protocol as described in the literature.[1] BLIP mutants (Y50A, E73M and K74G) were purchased from GenScript (Nanjing, China).

Native and ion mobility mass spectrometry. The proteins were buffer exchanged into 50 mM ammonium acetate by an Amicon 10K centrifugal filter before MS analysis. Native mass spectra were acquired on a Synapt G2Si mass spectrometer (Waters, Milford, MA) with house-made nanoESI emitters. 3-5 μL protein solution (5-30 μM in 100 mM ammonia acetate) was loaded into the nanoESI emitter and sprayed under the following conditions: capillary voltage 1.5-2.0 kV, source temperature 25 °C, trap and transfer collision energy 15 V, trap DC bias 45, trap gas flow 4-8 ml/min. Ion mobility measurements were carried out using the same equipment under the following conditions: IMS gas flow 30 ml/min, wave velocity 650 m/s, wave height 40 V and pressure 0.9 mbar. Drift time was extracted manually using MassLynx 4.1 and Microsoft Excel.

Hydrogen deuterium exchange mass spectrometry. For preparation of β-lactamases complexes with BLIP, 30 μM of β-lactamases was incubated with BLIP at a molar ratio of 1:1, 1:4.3 and 1:2.2 for TEM1/BLIP, SHV1/BLIP and PC1/BLIP, respectively. BLIP mutants with enhanced binding affinity were incubated with β-lactamases at a molar ratio of 1:1 (more than 90% bound). Percentage of the bound β-lactamases was calculated based on the concentration of β-lactamases bound to BLIP and K_d.[2] The mixtures were incubated on ice for at least 30 min before further experiments. Deuterium exchange was initiated by diluting 2 μL protein sample (20-30 μM) into 38 μL D_2O (99.9%, Cambridge Isotope Laboratories) buffer (100 mM phosphate buffer, pD 7.4). The proteins were deuterated for 60 sec and 10 min for local HDX (optimized from global exchange for 10 sec, 60 sec, 10 min and 60 min) and the exchange reactions were quenched by addition of a quenching buffer (10 mM phosphate buffer, 6% formic acid) to reach a pH value of around 2.5. 50 μL quenched solution was injected into a Waters nanoACQUITY UPLC system at 0 °C. After online pepsin digestion (Waters BEH pepsin column, 300Å, 5 μm, 2.1 mm x 30 mm) and desalting (Waters BEH C18 trap column, 130 Å, 5 μm, 300 μm × 50 mm) for 3 min at 100 μL/min, the peptides were eluted through a Waters UPLC BEH C18 column (130Å, 1.7 μm, 2.1

mm × 100 mm) with linear acetonitrile gradient (5-40%, 0.2% formic acid) at 60 µL/min. The pepsin column was washed 3 times between injections by a denaturing buffer (1.5M guanidine hydrochloride, 4% acetonitrile, 0.8% formic acid, pH 2.5). Global HDX was determined without pepsin digestion, and proteins were eluted with constant mobile phase (50% acetonitrile, 0.2% formic acid). Mass spectra were recorded using the Waters Synapt G2Si mass spectrometer in MS^e mode at 50-2000 Da. Three replicates were performed for each β-lactamase.

Data analysis for HDX-MS. Peptide lists were generated by Waters ProteinLynx Global Server (PLGS). The peptides fulfilled the following thresholds were processed with Waters DynamX 3.0 followed by manual inspection. Maximum mass errors: 10 ppm; Maximum sequence length: 20; Minimum PLGS score: 7; The minimum intensity: 10000; Retention time root standard deviation: 5%. Peptides of interest were eluted from 3-8 min with an average length of 13. The average mass error for all the peptides for analysis was below 3 ppm. The average standard deviation of the deuterium uptake was below 0.1 Da. Back exchange was estimated to be an average rate of 35% by analyzing fully deuterated peptides from digested PC1 (Fig. S7) and was not corrected when doing the comparison. The fractional deuterium uptake was calculated as reference to the maximum exchangeable amide hydrogens. Difference in deuterium uptake with 95% confidence interval (CI) was considered as a significant change for differential HDX. Uptake figures were produced by Microsoft Excel and relative deuterium uptake was mapped onto the crystal model of proteins using PyMol 2.0.7 (Schrodinger, LLC). Experimental details are summarized in Table S1 as suggested by a recent HDX-MS white paper.[3]

MD simulation of β-lactamases and of their complexes with BLIP. For the simulation of TEM1, SHV1 and PC1, the initial structures were directly obtained from protein data bank. The free and bound TEM1 were constructed from PDB IDs, 1btl and 1jtg, while SHV1 from PDB IDs, 1shv and 2g2u. The crystal structure of PC1 (PDB ID: 3blm) was used for the protein-only simulation. The initial structure of the PC1/BLIP complex was prepared by homology modeling using Modeller version 9.[4] The complex model was constructed using the crystal structures of apo-PC1 (PDB ID: 3blm) and the TEM1/BLIP (PDB ID: 1jtg), SHV1/BLIP (PDB ID: 2g2u) and KPC2/BLIP (PDB ID: 3e2l) complexes as templates. The β-lactamase in its free and bound states were subjected to molecular dynamics simulation at consistent parameters using GROMACS 5.1 series[5] with the Charmm27 all-atom force field. The protein atomic coordinates were encased in an octahedral or cubic box with a 1 nm-thick wall followed by solvation using the TIP3P water model. The charges on the protein were neutralized by adding Na^+ and Cl^- to 150 mM. Following energy minimization and 900 ps of restrained equilibration (100 ps under constant number, volume and temperature (NVT) and 800 ps under constant number, pressure and temperature (NPT), with progressively reducing restraints from 1000 to 0.1 kJ mol^{-1} nm^{-1}, 10 ns of unrestrained molecular dynamics simulations were performed. The time step was 2 fs and configurations were saved every 10 ps. All trajectories were subjected to evaluation by calculating the root mean square deviation (RMSD) of Cα positions reference to the energy-minimized structure and further analyzed by calculating their root mean square fluctuation (RMSF) of backbone positions for the last 5 ns.

TABLE S1. Summary of the details for the HDX experiments

| Data Set	Free TEM1	TEM1 bound with BLIP-WT	TEM1 bound with BLIP-Y50A
HDX reaction details	100 mM phosphate buffer in 95% D_2O, pH 7.4, RT	100 mM phosphate buffer in 95% D_2O, pH 7.4, RT	100 mM phosphate buffer in 90% D_2O, pH 7.4, RT
HDX time course (min)	1, 10		
Number of peptides	84	83	85
Sequence coverage	90%	90%	94%
Average peptide length / Redundancy	13.2 / 4.6	13.2 / 4.6	13.3 / 4.5
Replicates (biological or technical)	3	3	3
Repeatability	0.075 Da	0.037 Da	0.032 Da
Significant differences in HDX (ΔHDX)	NA	0.29 Da (95% Confidence Interval)	0.21 Da (95% Confidence Interval)
Data Set	Free SHV1	SHV1 bound with BLIP-WT	SHV1 bound with BLIP-E73M
HDX reaction details	100 mM phosphate buffer in 95% D_2O, pH 7.4, RT	100 mM phosphate buffer in 95% D_2O, pH 7.4, RT	100 mM phosphate buffer in 90% D_2O, pH 7.4, RT
HDX time course (min)	1, 10		
Number of peptides	61	28	61
Sequence coverage	89%	89%	90%
Average peptide length / Redundancy	12 / 3.7	12 / 1.2	12 / 3.2
Replicates (biological or technical)	3	3	2
Repeatability	0.057 Da	0.054 Da	0.028 Da
Significant differences in HDX (ΔHDX)	NA	0.26 Da (95% Confidence Interval)	0.24 Da (95% Confidence Interval)
Data Set	Free PC1	PC1 bound with BLIP-WT	SHV1 bound with BLIP-K74G
HDX reaction details	100 mM phosphate buffer in 95% D_2O, pH 7.4, RT	100 mM phosphate buffer in 95% D_2O, pH 7.4, RT	100 mM phosphate buffer in 90% D_2O, pH 7.4, RT
HDX time course (min)	1, 10		
Number of peptides	56	34	41
Sequence coverage	89%	89%	100%
Average peptide length / Redundancy	12 / 2.9	12 / 2.1	12 / 2.7
Replicates (biological or technical)	3	3	3
Repeatability	0.047 Da	0.076 Da	0.101 Da
Significant differences in HDX (ΔHDX)	NA	0.46 Da (95% Confidence Interval)	0.55 Da (95% Confidence Interval)
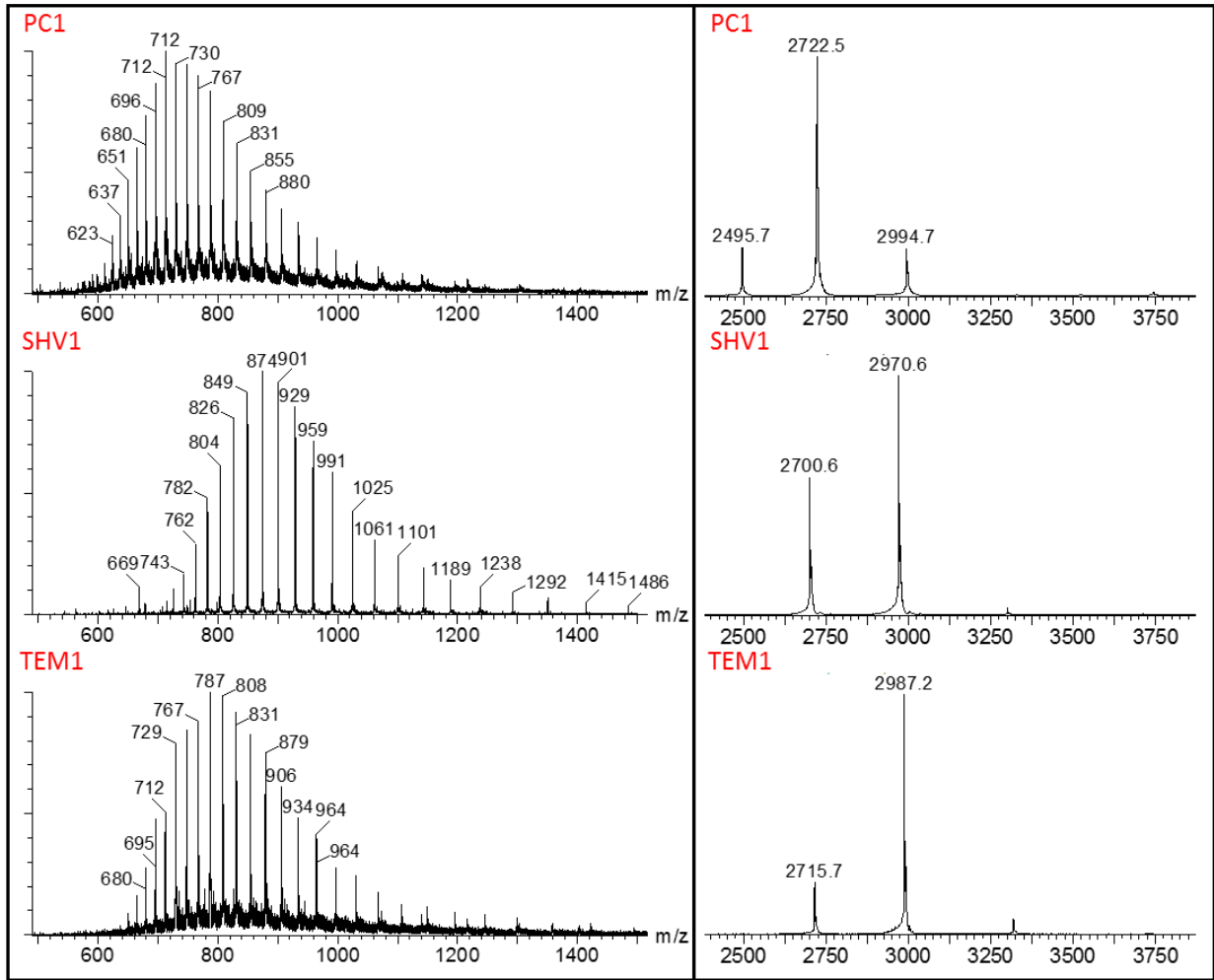
Fig. S1 Mass spectra of β-lactamases under denatured conditions (50% acetonitrile with 0.2% formic acid, left) and native conditions (100 mM ammonia acetate, right).
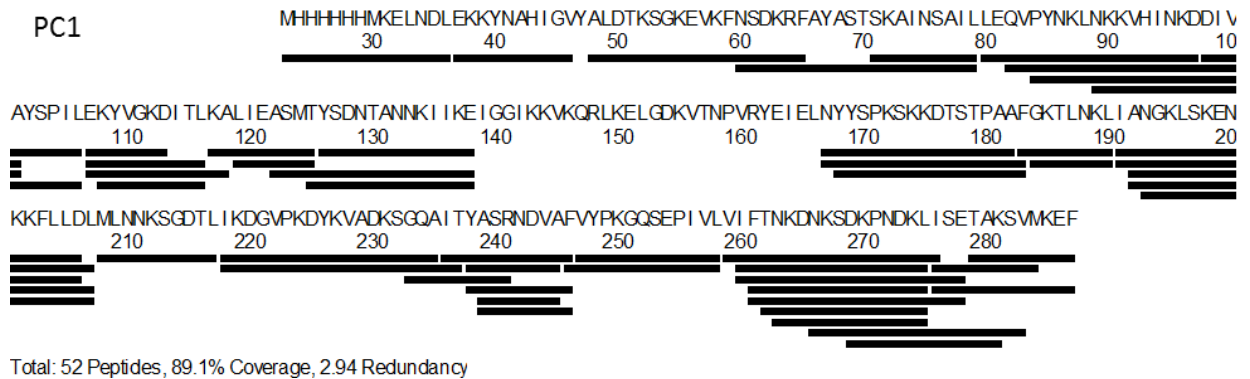
TEM1

MHPETLVKVKDAEDQLGARVGYIELDLNSGKILESFRPEERFPMMSTFKVLLCGAVLSRVDAGQEQLGRRIHYSQN
　　30　　　　　40　　　　　50　　　　　60　　　　　70　　　　　80　　　　　90　　　　　10

DLVEYSPVTEKHLTDGMTVRELCSAAITMSDNTAANLLLTTIGGPKELTAFLHNMGDHVTRLDRWEPELNEAIPNDERDTTMPAAMATTLRKLLTGELLT
　　110　　　　120　　　　130　　　　140　　　　150　　　　160　　　　170　　　　180　　　　190　　　　20

LASRQQLIDWMEADKVAGPLLRSALPAGWFIADKSGAGERGSRGIIAALGPDGKPSRIVVIYTTGSQATMDERNRQIAEIGASLIKHWHHHHHH
　　210　　　　220　　　　230　　　　240　　　　250　　　　260　　　　270　　　　280　　　　290

Total: 83 Peptides, 90.0% Coverage, 4.52 Redundancy

SHV1

MSPQPLEQIKLSESQLSGRVGMIEMDLASGRTLTAWRADERFPMMSTFKVVLCGAVLARVDAGDEQLERKIHYRQC
　　30　　　　　40　　　　　50　　　　　60　　　　　70　　　　　80　　　　　90　　　　　10

DLVDYSPVSEKHLADGMTVGELCAAAITMSDNSAANLLLATVGGPAGLTAFLRQIGDNVTRLDRWETELNEALPGDARDTTTPASMAATLRKLLTSQRLS
　　110　　　　120　　　　130　　　　140　　　　150　　　　160　　　　170　　　　180　　　　190　　　　20

ARSQRQLLQWMDDRVAGPLIRSVLPAGWFIADKTGAGERGARGIVALLGPNNKAERIVVIYLRDTPASMAERNQQIAGIGAALIEHWQRHHHHHH
　　210　　　　220　　　　230　　　　240　　　　250　　　　260　　　　270　　　　280　　　　290

Total: 71 Peptides, 88.6% Coverage, 3.73 Redundancy

PC1

MHHHHHHMKELNDLEKKYNAHIGVYALDTKSGKEVKFNSDKRFAYASTSKAINSAILLEQVPYNKLNKKVHINKDDIV
　　30　　　　　40　　　　　50　　　　　60　　　　　70　　　　　80　　　　　90　　　　　10

AYSPILEKYVGKDITLKALIEASMTYSDNTANNKIIKEIGGIKKVKQRLKELGDKVTNPVRYEIELNYYSPKSKKDTSTPAAFGKTLNKLIANGKLSKEN
　　110　　　　120　　　　130　　　　140　　　　150　　　　160　　　　170　　　　180　　　　190　　　　20

KKFLLDLMLNNKSGDTLIKDGVPKDYKVADKSGQAITYASRNDVAFVYPKGQSEPIVLVIFTNKDNKSDKPNDKLISETAKSVMKEF
　　210　　　　220　　　　230　　　　240　　　　250　　　　260　　　　270　　　　280

Total: 52 Peptides, 89.1% Coverage, 2.94 Redundancy

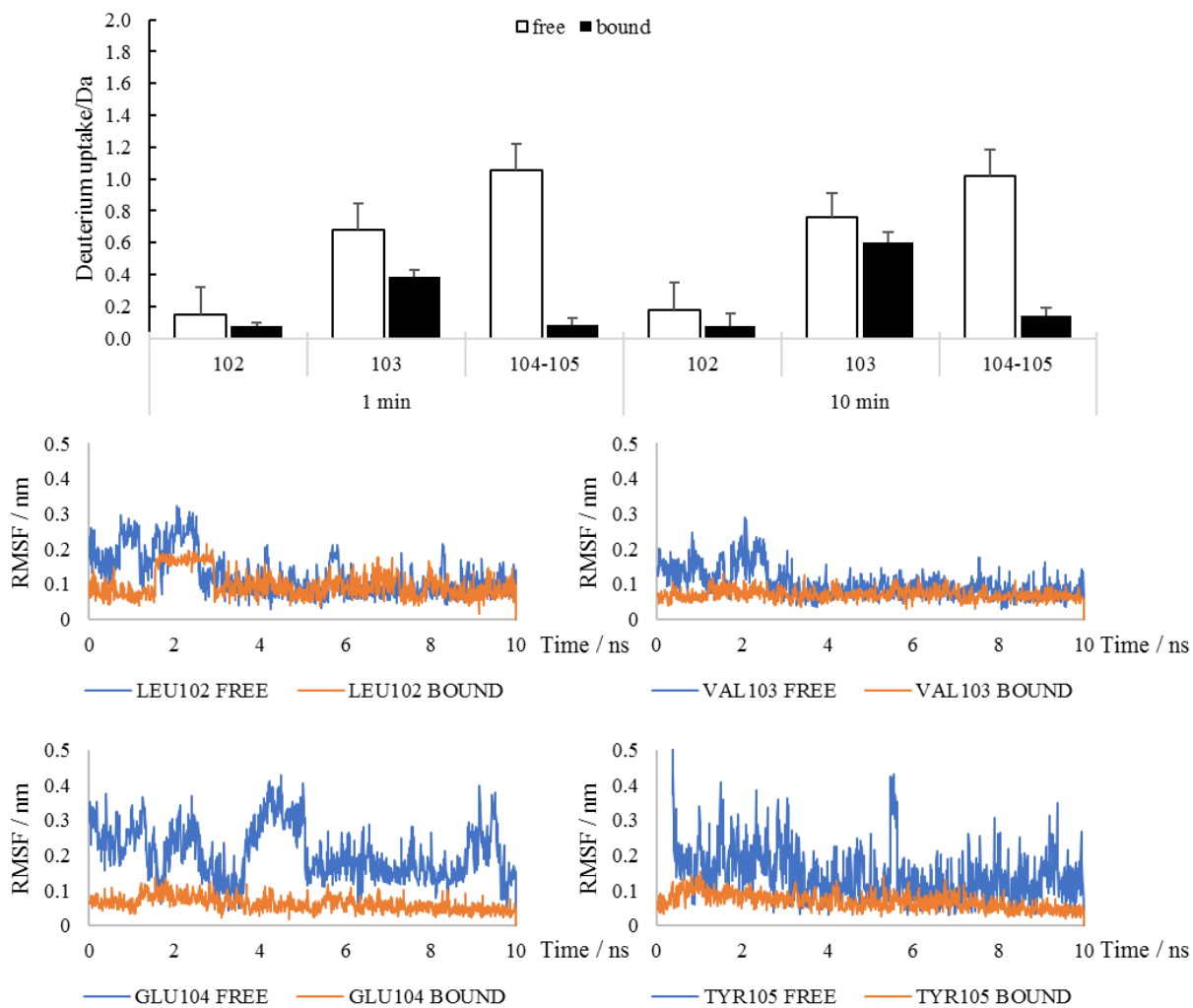Fig. S2 Sequence coverage of identified fragments from TEM1, SHV1 and PC1.

Fig. S3 Residue-level dynamics for the protruding loop measured by HDX-MS and MD simulation.
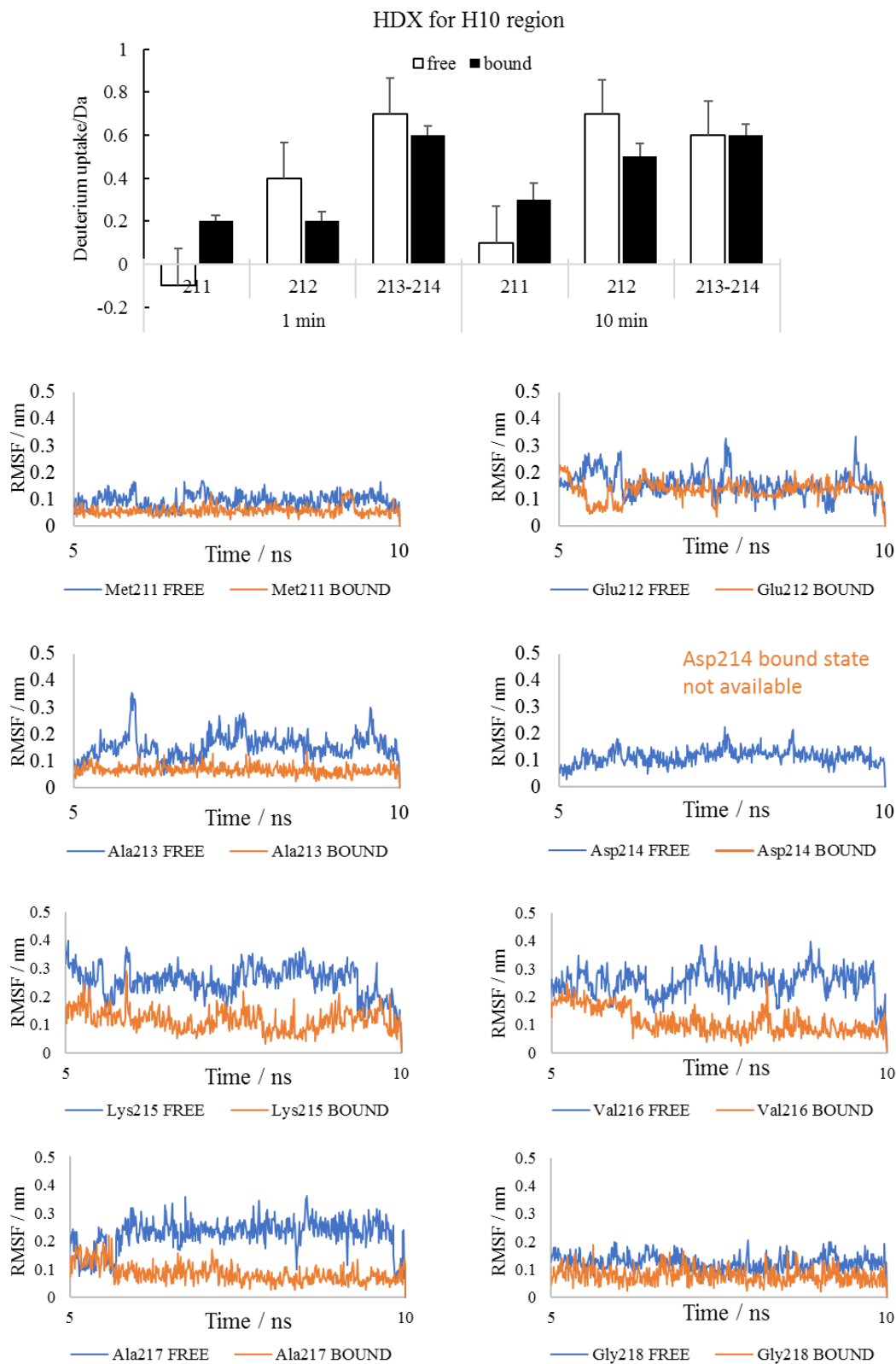
Fig. S4 Residue-level dynamics for the H10 region measured by HDX-MS and MD simulation. Error bars indicate standard deviations for the time points 1 and 10 min (n=3).
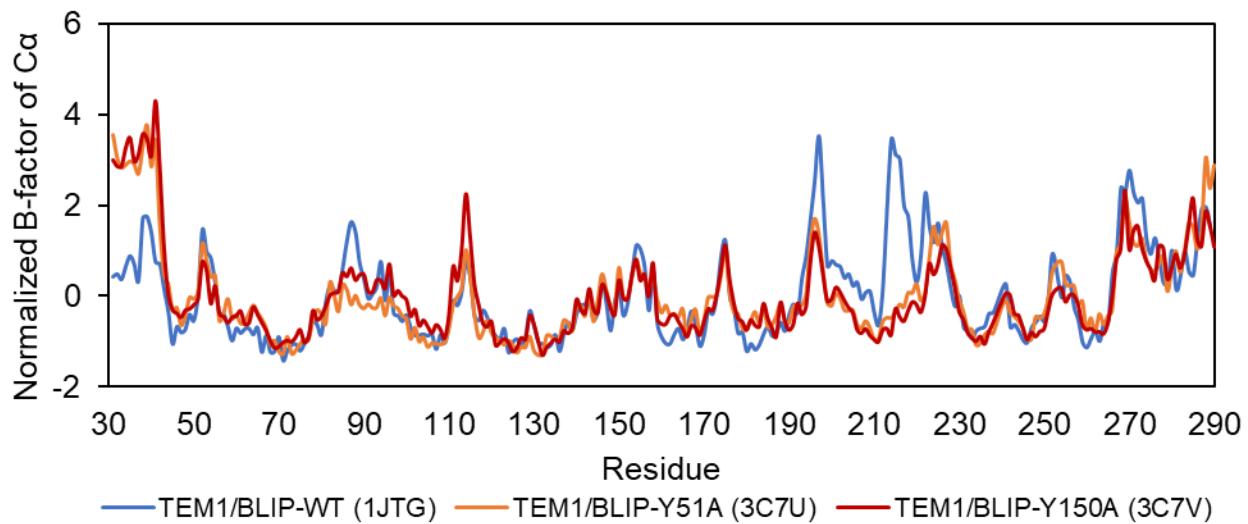
Fig. S5| Normalized B-factors of α-carbon for the bound states of TEM1 with BLIPs. The PDB IDs for obtaining the B-factors are shown in the parentheses.
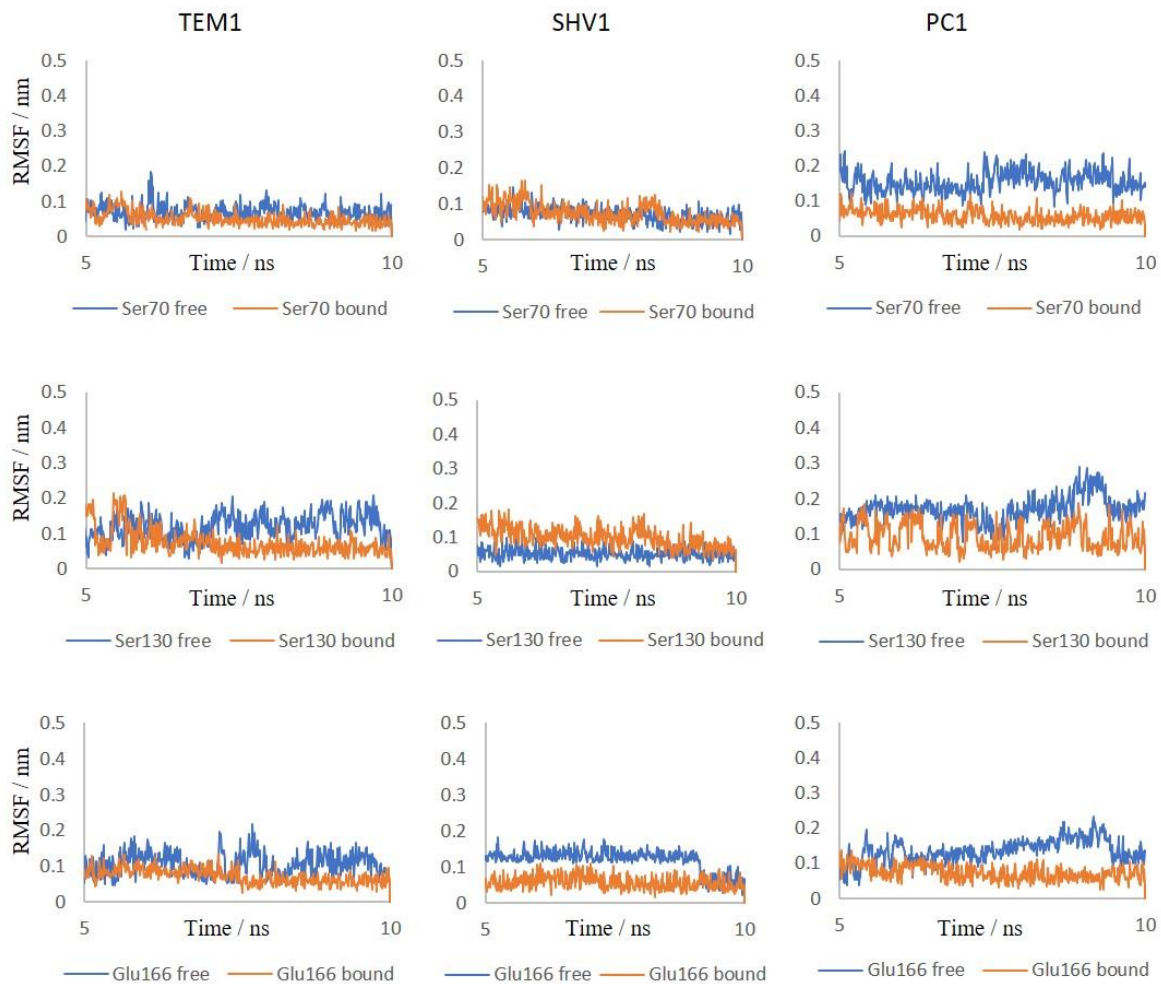
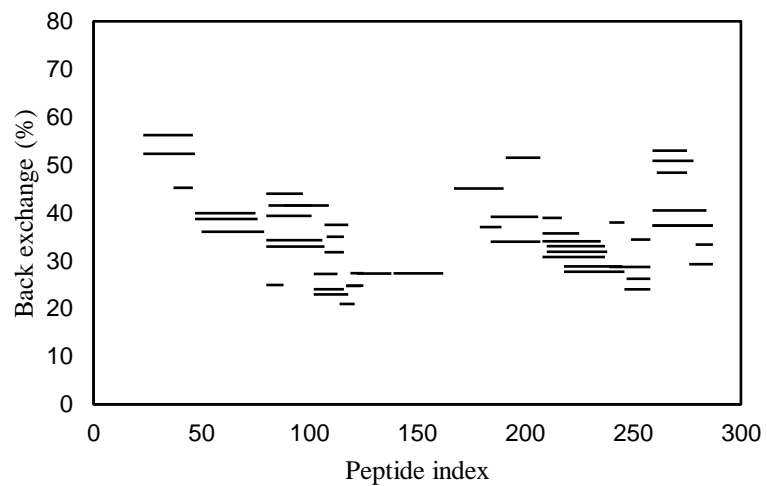Fig. S6 Residue-level RMSF (nm) for the catalytic sites of TEM1, SHV1 and PC1 measured by MD simulation.

Fig. S7 Back exchange of fully deuterated peptides from PC1.

References

1. Law, K.-H.; Tsang, M.-W.; Wong, Y.-K.; Tsang, M.-S.; Lau, P.-Y.; Wong, K.-Y.; Ho, K.-P.; Leung, Y.-C. Efficient Production of Secretory Streptomyces Clavuligerus β-Lactamase Inhibitory Protein (BLIP) in Pichia Pastoris. *Amb Express* **2018**, *8*, 64.

2. Mandell, J., Falick, A., Komives, E. Identification of protein-protein interfaces by decreased amide proton solvent accessibility. *Proc. Natl. Acad. Sci. USA.* **1998**, 95, 14705-14710.

3. Masson, G., Burke, J., Ahn, N., Anand, G., Borchers, C., Brier, S., Bou-Assaf, G., Engen, J., Englander, S., Faber, J., Garlish, R., Griffin, P., Gross, M., Guttman, M., Hamuro, Y., Heck, A., Houde, D., Iacob, R., Jørgensen, T., Kaltashov, I., Klinman, J., Konermann, L., Man, P., Mayne, L., Pascal, B., Reichmann, D., Skehel, M., Snijder, J., Strutzenberg, T., Underbakke, E., Wagner, C., Wales, T., Walters, B., Weis, D., Wilson, D., Wintrode, P., Zhang, Z., Zheng, J., Schriemer, D., Rand, K. Recommendations for Performing, Interpreting and Reporting Hydrogen Deuterium Exchange Mass Spectrometry (HDX-MS) Experiments *Nat. Methods* **2019**, *16*, 595-602.

4. Eswar, N.; Webb, B.; Marti-Renom, M. A.; Madhusudhan; Eramian, D.; Shen, M.; Pieper, U.; Sali, A. Comparative Protein Structure Modeling Using Modeller *Curr. Protoc. Bioinform.* **2006**, *15*, 5.6.1-5.6.30.

5. Pronk, S.; Páll, S.; Schulz, R.; Larsson, P.; Bjelkmar, P.; Apostolov, R.; Shirts, M. R.; Smith, J. C.; Kasson, P. M.; van der Spoel, D.; Hess, B.; Lindahl, E. GROMACS 4.5: A High-Throughput and Highly Parallel Open Source Molecular Simulation Toolkit. *Bioinformatics* **2013**, *29*, 845-854.